Chemical Reactions and Solvation at Liquid Interfaces: A Microscopic Perspective

Ilan Benjamin

Department of Chemistry, University of California, Santa Cruz, California 95064

Received September 5, 1995 (Revised Manuscript Received November 9, 1995)

Contents

Ilan Benjamin was born in Israel in 1956. He received his B.Sc. in chemistry and physics from the Hebrew University of Jerusalem. He received his Ph.D. in theoretical chemistry in 1986, working under the direction of Professor Raphael Levine at the Hebrew University of Jerusalem. His thesis work was on the development of Lie algebraic techniques for the study of molecular structure and spectra. He was a Weizmann Postdoctoral Fellow at the University of Pennsylvania, working on statistical mechanical models of vibrational relaxation. He also held a postdoctoral position at the University of California at San Diego, studying chemical reaction dynamics by computer simulations. In 1989, he joined the faculty at the University of California at Santa Cruz, where he is currently an Associate Professor of physical chemistry. In 1995–1996, he was a visiting professor at the Weizmann Institute of Science, Israel. Benjamin's research interests include the theoretical and computational studies of relaxation processes and chemical reaction dynamics in the condensed phase. In recent years, his research has focused on chemical reactions and solvation at liquid interfaces.

I. Introduction

The study of chemical reactivity at liquid interfaces occupies an important place in chemistry. Corrosion and the operation of electrochemical and photoelectrochemical cells are examples of chemical processes at the liquid/solid interface.[1,2] Electron transfer, ion transfer, and proton transfer at the interface between two immiscible liquids are fundamentally important for understanding processes such as liquid chromatography, phase-transfer catalysis,[3] drug delivery problems in pharmacology,[4] and other phenomena in membrane biophysics.[5] The uptake of pollutants by water clouds, an important atmospheric phenomenon,[6] involves reactions such as ionization at the water liquid/vapor interface. Understanding the behavior of solute molecules and their reactivity at the interface between a liquid and a second phase is not only important because of its direct relevance to the processes mentioned above. This study is also important at the fundamental/theoretical level, as the inhomogeneous environment is characterized by a number of unique properties that are expected to influence the behavior of a chemically active system in a way that is significantly different from the behavior in bulk liquid or in the gas phase.

The study of chemical reaction dynamics and thermodynamics and the related processes of solvation and adsorption at liquid interfaces goes back to at least the beginning of the century. Most of these studies employed indirect techniques that typically involved measurements of macroscopic properties such as surface tension and surface potential.[7] Although these techniques are able to elucidate many of the important factors that influence chemical reactivity at liquid interfaces, they lack the ability to provide a detailed understanding at the microscopic level. In recent years, progress in three different areas has significantly helped to alleviate this shortcoming.

First, advances in a number of new experimental techniques enable workers to gain unprecedented sensitivity and selectivity in the measurements of interfacial phenomena. Nonlinear optical techniques such as second-harmonic generation (SHG) and sum frequency generation (SFG)[8] are able to explore the liquid/vapor interface[9] and buried interfaces, such as

S0009-2665(95)00230-5 CCC: $25.00

liquid/liquid[10,11] and liquid/solid interfaces,[12,13] by taking advantage of the fact that the signal is produced mainly by molecules in the interfacial region.[8] These techniques have been extensively used in the last 5 years to study a large number of systems including solvation,[14] isomerization,[15] ionization,[16−19] adsorption,[20−25] energy transfer[26] and electron transfer,[27] vibrational spectroscopy,[28−30] and structure[10,11,31−35] at liquid interfaces. In addition to these surface-specific techniques, other methods that have been used to study bulk systems have been adapted to the study of interfaces. Light scattering[36−38] has been extensively used in the study of the liquid/vapor interface of many fluids. Neutron scattering[39] has been used to study oil/water interfaces. Fluorescence anisotropy decay[40,41] has provided data on the molecular nature of water/alkane interfaces. A nanometer-sized tip electrode has been used to carry out electrochemical measurements at the solution−polymer interface.[42] Infrared spectroscopy in a total reflection geometry has provided valuable insight into adsorption at the liquid/liquid interface.[43] Many excellent reviews of the above techniques and their applications to liquid interfaces are available, and we refer the reader to these articles for additional information.[8,9,11,44,45]

Second, recent experimental[46] and theoretical[47,48] studies of bulk liquid chemical reaction dynamics demonstrate the importance of the molecular structure of the liquid in influencing and modifying the simple gas-phase behavior. These research efforts show that we can no longer be satisfied by a picture that portrays the solvent as a structureless medium, and that the effect of the liquid must be considered at the microscopic level. We will see that this is particularly important for understanding interfacial phenomena, as the interfacial region itself is only a few molecular diameters thick. Throughout this review, we will make use of results obtained for chemical reaction dynamics in bulk liquids, and the reader is referred to the reviews listed in the beginning of this paragraph for details.

Finally, advances in statistical mechanical theories[49−52] and computer simulations[53] of pure inhomogeneous liquids has contributed significantly in recent years to our theoretical understanding of the microscopic structure and dynamics of the neat interface. While progress in the statistical mechanical theories has mainly been limited to calculating a small number of properties (such as density profile and surface tension) of simple inhomogeneous liquids, computer simulations have provided additional complex structural and dynamical information for both simple and complex interfacial systems, as will be discussed in details below.

The purpose of this paper is to review the microscopic insight that has been gained in recent years into solvation and reactions at liquid interfaces. Since most of what is known theoretically has been obtained by computer simulation, the review will be heavily biased toward results obtained using this technique. The goal of the review is to present unifying concepts for describing solvation and reactions at the three liquid interfaces (liquid/vapor, liquid/liquid, and liquid/solid), focusing on results that are not too specific for a given system, and referring the reader to the appropriate literature for technical details.

Thus, we start this review with a summary of the unique properties of liquid interfaces and a discussion of the way these properties are expected to influence reactivity and solvation. We stress the fact that in many cases the effect of the inhomogeneous environment is such that the system exhibits qualitatively different behavior from the one in the bulk. This part of the review will serve as the necessary background for the rest of the paper. It will be limited to a brief exposition, as there are a number of reviews on the microscopic description of the neat liquid interface (experimentally and theoretically).[44,53,54] Technical details about the computations and about the potential energy surfaces will be kept to a minimum.

We then discuss a number of general types of reactions: isomerization reactions, solvation, ion transfer, and electron-transfer reactions. Each of these topics will be discussed from both the static and dynamic perspective, with an emphasis on the general effect of the inhomogeneous environment, rather than on the specifics of a given interfacial system.

II. Uniqueness of Liquid Interfaces—General Concepts

The liquid interfacial region is characterized by several nonuniform thermodynamic properties such as density, viscosity, and dielectric response,[44,49,50,55] as well as by a unique molecular structure and dynamics. Obviously, a knowledge of these properties is crucial for the correct interpretation of experimental data, for the development of simple models of the inhomogeneous region, and for the design of new experiments. The summary below is based on the results of molecular dynamics and Monte Carlo simulations of the neat interfacial system, on statistical mechanical theories, and on experimental data. In order to keep this review to a reasonable size, technical details about the techniques used to obtain this data will be omitted, and the reader is referred, in each case, to the appropriate papers and reviews.

A. Density of Liquids at Interfaces

The coexistence of two different phases with two different bulk densities necessarily results in a change in the density as one moves from one phase to the next. This density profile has been the main focus of a variety of theoretical treatments, including mean field theories,[50] integral equations, and classical density functional theory.[52] Experimentally, the density profile of the liquid in contact with a second phase can be determined directly by light-scattering techniques,[36,37] and indirectly by spectroscopy[45] and other means.[7]

Perhaps the most direct and straightforward information about the density variation at liquid interfaces has been obtained by Monte Carlo and molecular dynamics simulations of liquid/vapor,[50,56−67] liquid/liquid,[68−77] and liquid/solid interfaces.[78−88] All of the above theoretical, computational, and experimental techniques give a consistent picture of the

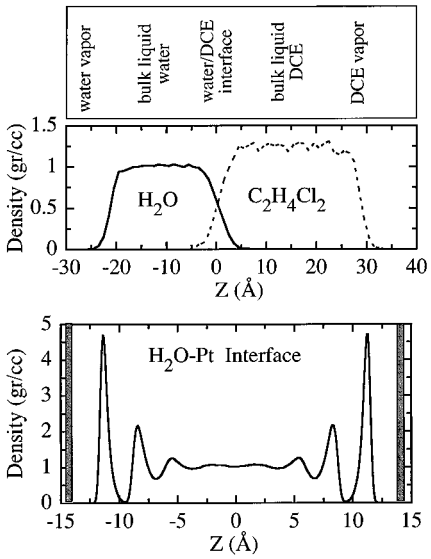

Figure 1. Density variations at several liquid interfaces. In the top panel the density profiles of water and of 1,2-dichloroethane at the liquid/liquid interface and the liquid/vapor interface are shown (from the result of 200 ps molecular dynamics trajectories in a system that includes 343 water molecules and 108 DCE molecules). In the bottom panel, the density of water between two parallel Pt (100) surfaces is shown (from a 1 ns molecular dynamics trajectory with 512 water molecules). In both cases, the temperature is 300 K.

density behavior at these interfaces, which we now summarize with the help of Figure 1, which presents examples of these three interfacial regions.

For most liquids at equilibrium with their vapors far below the critical point, the density monotonically changes from the value in bulk liquid to that of the bulk vapor over a distance of a few molecular diameters—4−10 Å. This finite and sharp width is the result of the superposition of thermally excited capillary waves.[50,51] Capillary wave theory gives the following relationship between the width and the macroscopic surface tension of the liquid:[50,89]

$$\sigma^2 = (4\pi\beta\gamma)^{-1} \ln\frac{1 + (2\pi l_c/\xi_b)^2}{1 + (2\pi l_c)^2/S} \qquad (1)$$

In this equation, the width σ is the mean-squared deviations of the local surface heights (h) from their average, ($\langle h\rangle$), assuming that they are Gaussian distributed: $P(h) = (2\pi\sigma^2)^{-1/2}e^{-h^2/2\sigma^2}$. The length scale $l_c = [\gamma/g(\rho_A - \rho_B)]^{1/2}$ is called the capillary length, γ is the surface tension, S is the surface area of the liquid, g is earth's gravity and $\beta = 1/kT$. ρ_A and ρ_B are the bulk densities of the two phases. The capillary length is on the order of a few millimeters for water at room temperature. The bulk correlation length, ξ_b, is a few molecular diameters for most liquids far below their critical point. For water at room temperature, it is about 5 Å. Thus, for a microscopic sized sample, we have: $\sigma^2 = (4\pi\beta\gamma)^{-1} \ln S/\xi_b^2$. Note that the interface width exhibits logarithmic divergence as $g \rightarrow 0$ and $S \rightarrow 0$. That is, gravity is necessary to establish an interface between two fluids in the thermodynamic limit.

The density profile predicted by the capillary wave theory is given by

$$\varrho(z) = \frac{1}{2}(\varrho_A + \varrho_B) - \frac{1}{2}(\varrho_A - \varrho_B)\mathrm{erf}\left(\frac{z - \langle h\rangle}{\sqrt{2}\sigma}\right) \qquad (2)$$

where erf is the standard error function. Other models of the interface give rise to similar density profiles. For example, the classical van der Waals mean field theory gives rise to a tanh dependence instead of the error function.[50] In addition to the width σ, a more common parameter for describing interface width is the so-called 10−90 thickness[36] (t_s), which is the region where the density of the liquid changes from 10% to 90% of the bulk value. The interface location $\langle h\rangle$ is the point where the density is the average density of the two phases. A closely related definition, used extensively in the thermodynamic description of liquid interfaces and independent of any model of the interface, is the Gibbs dividing surface. For a one-component system, this is the location along the interface normal where the decrease in the number of molecules on the liquid side (relative to the number expected if the density stayed at the bulk value) is exactly balanced by the increase on the vapor side. For water at room temperature, the Gibbs surface is near the position in which the average water density is 0.5 g/cm^3.

The basic predictions of capillary wave theory have been confirmed in experiments[36,90] and simulations.[53] For example, the Gaussian distribution of local interface positions has been examined in detail[68,74,76] and found to hold down to a surface area of ξ_b^2. A procedure for deriving a capillary wave Hamiltonian, which provides a rigorous justification for these calculations, has been discussed by Weeks.[91] Other issues related to the microscopic foundation of this model and its scaling behavior in different limits have been discussed,[92−94] but they are outside the scope of this review.

The top panel of Figure 1 shows the results of a molecular dynamics simulation of the water/1,2-dichloroethane (DCE) interface in a simulation box geometry that allows for the establishment of a liquid/liquid interface in the center of the simulation box and a liquid/vapor interface for each of these two liquids. The water is described here using a flexible SPC model, and the DCE is described using a four-center, simple charge, flexible model.[74] The general shape of the density profile at the liquid/vapor interface is close to the expression given by capillary wave theory. The shape of the liquid/liquid interface is also very similar. Note that the width of the liquid/liquid interface is greater than that of the water liquid/vapor—consistent with the higher tension of the latter surface. This surface tension can be directly calculated from the molecular dynamics trajectories and this can be employed as a test of the potential energy surfaces used in the simulations. Details about the theory[49] and examples of calculations at the liquid/vapor and liquid/liquid interfaces can be found in the references listed at the beginning of this section.

Although the monotonic change in the densities is common to many liquids, (with the exception of the liquid/vapor interface of liquid metals[95,96]), there is evidence from molecular dynamics simulations[74−77] for dampened oscillations in the densities on the bulk

side of the liquid/liquid interfacial region. However, it is not clear that these oscillations are a real physical aspect of the system or an artifact of the small system size and short simulation time. For example, Toxvaerd and Stecki found (using molecular dynamics simulations) stable equilibrium oscillatory structures in the density profiles of two immiscible Lennard-Jones liquids, but these vanish with the increase in the surface area.[77]

A qualitatively different situation arises at the interface between a liquid and a solid. The relative immobility of the solid atoms imposes geometrical constraints on the packing of the solvent molecules in the few layers next to the wall. This results in an oscillatory density profile which decays to the constant bulk value after several molecular diameters, as shown by many computer simulations,[78−88] statistical mechanical theories,[52,97,98] the measurements of forces between surfaces in liquids,[99−101] and other experimental observations.[102] The decay length of the oscillations depends on the type of intermolecular forces and it seems to be larger for simple nonpolar liquids than for water. As an example, in the bottom panel of Figure 1 we show the density profile of water near the 100 surface of Pt, using a molecular dynamics simulation with 512 water molecules modeled using the SPC potential referred to earlier and the water/Pt potential developed by Spohr and Heinzinger.[81] Other models of water and solid surfaces, described in the references listed above, give qualitatively similar results.

Why should the density of liquid at interfaces be relevant for the study of solvation and reactions in these systems? We may distinguish two effects, a thermodynamical equilibrium one and a dynamical one.

For reactions that involve a significant change in the volume occupied by the reactants and products, density changes in bulk liquids and in compressed gases have marked effects on the free energy of the reactants, products, and the transition state, and thus on the equilibrium constant and the transition state theory rate constant.[103] Given the universal nature of density changes at liquid interfaces summarized above, one expects to see a manifestation of these equilibrium effects on reactions and on solvation at liquid interfaces.

From the dynamical point of view, a change in density is usually connected with a change in the viscosity of the medium. For example, the viscosity of vapor is much lower than the bulk liquid viscosity, and although no direct experimental data are available, there is evidence from molecular dynamics simulations that the diffusion constant in the plane perpendicular to the liquid/vapor interface is enhanced. At the liquid/solid interface, there are experimental data supporting a higher viscosity of the liquid film adsorbed on the solid surface.[104,105] As has been demonstrated by much experimental and theoretical work, a change in liquid viscosity may have an appreciable effect on the rate of the reaction.[47,106] If the rate-determining step is the activation (energy diffusion regime), then an increase in the viscosity of the solvent increases the rate. On the other hand, if activation is rapid, an increase in the viscosity may decrease the rate of the reaction by inducing recrossings in the transition state region, the extreme situation being that the crossing of the transition state may be a slow spatial diffusion process.[107]

B. Molecular Structure and Dynamics

At the microscopic level, the interfacial region is characterized by a strong asymmetry in the intermolecular interactions between the molecules. This results in a molecular structure and dynamics that may be significantly different from that in the bulk liquid. Figure 2 presents a sample of such properties. No attempt is made here to cover all the properties that have been measured or calculated. For a comprehensive survey the reader is referred to the references listed above.

1. Pair Correlation

The pair correlation function $\rho^{(2)}(\underline{r}_1,\underline{r}_2)$ is proportional to the probability of finding a particle at the

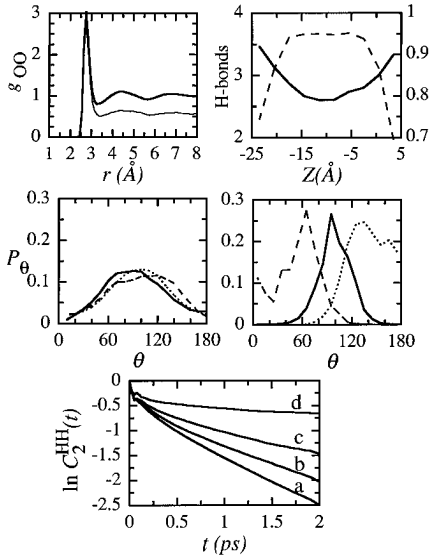

Figure 2. A summary of various structural and dynamical properties of water (300K) at interfaces. Top left panel: The oxygen−oxygen radial distribution function (thick line, bulk water; thin line, the water/1,2-dichloroethane interface). Top right panel: Hydrogen-bond statistics at the water/1,2-dichloroethane interface (the region between −5 and 5 Å), in bulk water (−15 Å < Z < −5 Å) and at the water liquid/vapor interface (Z < −15 Å) (dashed line, the average number of hydrogen bonds per water molecule (left x axis); solid line, the number of hydrogen bonds per water molecule divided by the coordination number of water in the same region). Center left panel: The probability distribution function for the angle between the water dipole moment and the normal to the interface. The solid, dashed, and dotted lines correspond to the interface between water and water vapor, water and 1,2-dichloroethane, and water and nonane, respectively. Center right panel: The probability distribution function for the angle between the water dipole moment and the normal to the platinum surface (solid line, uncharged metal; dashed line, the Pt surface is negatively charged; dotted line, the metal is positively charged). Bottom panel: The water molecule H−H vector reorientation time correlation function. The lines a−d correspond to water at the liquid/vapor interface, bulk water, water at the interface with 1,2-dichloroethane and the water layer next to an uncharged Pt surface, respectively.

position $\underline{r}_1$, given that there is a particle at the position $\underline{r}_2$. Thus, in contrast to the density profile, which gives information about the average distribution of particles in space (a so-called singlet property), this function gives information about the spatial correlation between the particles. In bulk liquids, because of translational and rotational invariance, $\rho^{(2)}$ is a function of the radial distance $r = |\underline{r}_2 - \underline{r}_1|$ only. At liquid interfaces, the spherical symmetry is broken, and so the pair correlation is now also a function of the locations z_1 and z_2 of the two particles relative to the interface. This 4-dimensional object is difficult to compute, and thus one is usually interested in an average over all locations within a finite interfacial zone.

The top left panel in Figure 2 shows the oxygen−oxygen pair correlation in bulk SPC water and the average pair correlation at the water liquid/vapor interface at the same temperature. Note that the first peak of the average pair correlation at the interface is very similar to the one in the bulk. This reflects similar first coordination structure. The difference between the two functions is mainly in the fact that at the interface there are, on average, fewer water molecules outside the main solvation shell. Thus, the second peak is almost not visible, and the asymptotic value of the function is close to 0.5 instead of 1. Note also that the total area under the first peak is somewhat reduced, reflecting that during the few hundred picosecond run, the first coordination shell of four water molecules may be missing one or two water molecules for part of the time. Although these details are specific to the water oxygen−oxygen correlation, calculations of other pair correlations in water and in other liquids show similar features. The tendency to keep the first coordination shell undisturbed as much as possible is most noticeable in polar and hydrogen-bonded liquids.[58,62,74] As the liquid becomes less polar, a significant reduction in the first peak can be observed, although the peak position is generally unaffected.[74]

2. Hydrogen Bonding

Hydrogen bonding is especially relevant to understanding water properties at interfaces because it is a sensitive measure of the surface environment. We define two water molecules to be hydrogen bonded if their mutual interaction energy is more negative than −10 kJ/mol. This is somewhat arbitrary, but it is possible to show that the conclusions below are independent of the precise definition. (Other definitions that have been used include an oxygen−oxygen distance being less than some cutoff.[68,71,74,108])

The top right panel of Figure 2 shows (in dashed line) the average total number of hydrogen bonds for a water molecule that is located in bulk water, at the water liquid/vapor interface, and at the water/DCE interface. We see that in bulk water, each water molecule is hydrogen bonded to an average of 3.6 water molecules, but at the water/DCE interface and the water liquid/vapor interface this number drops to a value between 3 and 2, depending on the exact location of the water molecule relative to the Gibbs dividing surface. An interesting result is obtained when this number is divided by the water's coordination number. The resulting quantity is indicated in the same panel with a solid line. It can be thought of as the fraction of the configuration in which a given hydrogen bond exists. One sees that this number is close to 0.9 at both interfaces, but is only 0.8 in the bulk. Thus, although there are fewer hydrogen bonds at the interface, they seem to last longer. Very similar results were found for other water/organic liquid interfaces.[68,76]

3. Molecular Orientation

The total intermolecular force on a given molecule at the interfacial region is strongly anisotropic. As a result, certain molecular orientations may be preferred at the interface. This property is of significant importance because steric requirements for chemical reactions at interfaces may lead to the strong dependence of reactivity on molecular orientation at the interface. Molecular orientation also determines liquid surface potential,[109] which is of fundamental importance in electrochemistry.[2] In addition to the density profile, molecular orientation is a property for which quite a large number of results have been obtained using statistical mechanical theories and experiments. An excellent review of this subject, which includes mainly theoretical, but also some experimental, work up until 1986 has been written by Gubbins.[110] Here we summarize some key results obtained in recent years, most of them for water.

The center left panel in Figure 2 shows the results of the molecular dynamics calculation of the probability distribution for the angle θ between the water electric dipole and the normal to the interface, for the water liquid/vapor interface, at the interface between water and DCE (a weakly polar liquid) and at the interface between water and nonane (a nonpolar hydrocarbon liquid). Despite the different nature of these interfaces, the distributions are quite similar. They are all broad and generally peaked around 90°, which corresponds to the water dipoles lying approximately parallel to the interface. Although these results were obtained using the SPC model for water, it is noteworthy that similar behavior is found using other water potentials. The similarity of the water dipole orientations in different systems probably reflects the fact that at this orientation the water is able to maximize hydrogen-bonding possibilities with other water molecules.

In contrast, more widely varying results are obtained for the orientation of the H−H vector using either theoretical[109−111] or simulational treatments[53,54,64] of the water liquid/vapor interface. A complicating feature, which can partially account for this fact, is discussed by Croxton,[111] who notes that the molecular orientation is very sensitive to the size and sign of the components of the water quadrupole moment. However, other differences in the model potentials can be important, as discussed by Zhu, Singh, and Robinson.[54]

Experimentally, water orientation at interfaces is difficult to measure. Until the introduction of nonlinear optical techniques, indirect methods such as surface potential measurements could not give unambiguous results. SHG experiments by Eisenthal

and co-workers on the neat water liquid/vapor interface[32] suggest that water dipoles point slightly toward the bulk, but that the angular distribution is very broad and the energy difference between the "up" and "down" orientations is only $0.5kT$.[112] However, the interpretation of the experiment depends on some unproven assumptions regarding the elements of the nonlinear susceptibility of water molecules. A more direct attempt to answer the related question of whether there are free OH bonds at the water surface was carried out by Shen and co-workers.[29,30] They used SFG to measure the vibrational spectrum of interfacial water and were able to identify the peak that corresponds to free OH bonds. Molecular dynamics calculations of the surface vibrational spectra using a flexible SPC model are in qualitative agreement with this result.[67] Despite this progress, the question of the orientation of water at interfaces is very much open. For example, it is not clear how important the effects of water polarizability and long-range forces, which are missing from most of the treatments discussed above, are (although there is some evidence that the inclusion of electronic polarizability does not change the structure significantly, but may slow down the molecular reorientation dynamics[63,113]).

Molecular orientation at interfaces can be affected by external perturbations. An example is shown in the right center panel of Figure 2 for the water/Pt interface. The solid line shows that when there is no external electric field, the water dipoles lay parallel to the interface, as in the previous examples. This is despite the fact that the water/Pt potentials are such that a single water molecule is adsorbed with an oxygen on top of a Pt atom (so that the water dipole is perpendicular to the interface), reflecting the tendency of water molecules to maximize hydrogen bonding. When an external electric field of an intensity of 1 V/Å is applied to the system (corresponding to a charge of 8.8 μC cm^{-2}), the peak of the distribution shifts in the expected direction depending on the sign of the charge on the metal. When the metal is positively charged, there is a significant population of water molecules whose dipoles point into the bulk water. When the metal is negatively charged, the competition between the water/Pt potential, the external field and the hydrogen bonding results in the dipole pointing toward the metal, but the normal direction is not as preferred as in the case of the positive charge. These results are similar to what has been observed by other studies of water near charged surfaces.[84,85,87] However, the quantum mechanical aspects of the bonding of the oxygen lone pair to the metal surface, as reflected by a modified work function, are still not well understood.[86]

Experimental and theoretical data on liquids at solid surfaces, and in particular, the water orientation at solid metallic and nonmetallic surfaces are widely available using a number of experimental techniques. Because this has been extensively reviewed in recent years, we refer the reader to these papers for details.[45,54,114]

4. Dynamics

Finally, we briefly consider the dynamics of liquids at interfaces. At the liquid/vapor and liquid/liquid interfaces, the available data mainly concern the macroscopic dynamics (capillary wave and hydrodynamics), but very little has been done on the microscopic dynamics such as molecular rotation. (The local diffusion and viscosity of liquid at interfaces was discussed earlier in this paper.) Thus, most of what is known about the microscopic dynamics has been obtained using molecular dynamics computer simulations. Relatively more information about molecular dynamics at the liquid/solid interface has become available in recent years through the application of new spectroscopic techniques.[45,114]

For water molecules at interfaces, it is generally observed that the dipole reorientation time is only mildly different at the interface from the value in the bulk.[74,83,115] Similarly, the H−H vector reorientation time (which determines the NMR line shape) is only slightly affected. Nevertheless, the variations in this quantity as one examines different interfaces are quite informative.

If $\hat{e}_r$ is a unit vector along the H−H vector in a water molecule (or along another molecule-fixed direction for other reorientations), then a measure of the reorientation time of this axis is provided by the time correlation function:

$$C_2(t) = \langle P_2[\hat{e}_r(t+\tau)\hat{e}_r(\tau)]\rangle \qquad (3)$$

where the angular brackets represent an ensemble average over all the water molecules in the interface region (or in the bulk) and over all time origins τ, such that τ is less than the residence time of the molecule in the given region. $P_2(x) = (3x^2\text{-}1)/2$ is the second Legendre polynome.

The bottom panel of Figure 2 shows the H−H reorientation time correlation function for water in different systems. The reorientation dynamic at the liquid/vapor interface is slightly faster than in the bulk, whereas at the water/DCE interface it is slightly slower than in the bulk. The first layer of water at the water/Pt surface is much less mobile in comparison. Although the actual numbers will vary depending on the potential energy surface of the water (for example, including electronic polarizability generally slows down the dynamics), the relative numbers seems to reflect the strength of the interaction between water and the second phase and the tendency of water to maximize the hydrogen-bonding network. It is interesting to note that there is evidence from molecular dynamics simulations that an external electric field which breaks down the hydrogen-bond network gives rise to a moderate acceleration in the molecular rotation and diffusion time.[54,116]

In addition to the single molecule dynamics, the dynamics of more global surface deformations at length scales just above the bulk correlation length may be of relevance to the behavior of a chemically interesting system. This will become more clear below when we discuss the issue of surface roughness. These surface deformations have been characterized at the water/DCE interface.[74] They can be thought of as transverse density fluctuations ("fingers"), whose dynamics are on the tens of picoseconds time scale.

All the data in Figure 2 were obtained from molecular dynamics simulations of several systems involving molecular liquids (mainly water). Although current statistical mechanical theories of inhomogeneous molecular liquids are able to calculate molecular orientation and give some limited information about the pair correlation,[52] more detailed structural and dynamical information is not available.

The unique molecular structure and dynamics are expected to influence solvation and reactions in a fundamental way, as will be demonstrated later in this paper. In many cases, the contribution of the solvent to the equilibrium and dynamic behavior of a chemically "interesting system" are coming mainly from the first few solvation shells. Thus, any change in the liquid structure at the interface may leave its signature in the structure of the solute solvation shell.

C. Dielectric Properties

An important macroscopic property of liquids at interfaces is their dielectric constant. Knowledge of this property is especially important for understanding the behavior of ions and polar solutes at liquid interfaces, and therefore a significant part of this review will deal with this issue. The dielectric constant and, more generally, the dielectric response, of a liquid at the interface reflect all of the unique interfacial microscopic characteristics discussed above. In general, the reduced orientational freedom (such as observed at the water/metal interface) and the reduced density (as in the liquid/vapor interface) result in a smaller dielectric constant than that in the bulk.

Because the dielectric response involves contributions from a large number of molecules that are spatially distributed at the interfacial region, it is a difficult quantity to calculate. Thus, although it is a routine matter to compute the dielectric constant and the frequency-dependent dielectric response for bulk liquids, no such calculations have been reported for liquids at interfaces. As a result our knowledge about this quantity is limited to indirect experimental information and simple models, whose consequences may be tested by comparison with experiments and simulations.

Typically, the dielectric constant is used in continuum electrostatic models of the interface in order to determine solvation free energies and the qualitative effects of the interface on the structure of adsorbed species and their interactions. One simple approach is to assume that the dielectric constant is equal to the bulk value up to a mathematically sharp interface, where it jumps to the constant bulk value of the second phase. This step-function model has been extensively used in the literature,[55,117] and it will be used later in this review. In this model, interfacial effects are simply the results of image charges that insure the continuous variation of the tangential component of the electric field across the interface. Another model used extensively in interfacial electrochemistry is based on the assumption that as far as the dielectric behavior is concerned, the interfacial region is a separate phase with a fixed dielectric constant, different from the values of the two bulk phases. Thus, a dielectric constant of 5−10 for the few water layers adsorbed on the metal electrode is used to explain capacity measurements and the spectroscopic line-shape shifts of adsorbed species.[1]

Given that the dielectric constant is a macroscopic continuum concept, it is expected that it will fail at some point for a system which is only a few molecular diameters in size. One way to push this concept down to microscopic sizes is to consider the dielectric constant a function of the distance from the interface, $\epsilon(Z)$. This dielectric profile can be used in continuum electrostatic models in a way similar to the use of a distance-dependent dielectric constant in bulk solvation models.[118] Near the liquid/gas critical point, where the interface is broad, $\epsilon(Z)$ may be expanded to linear order in z and used in analytical theories.[109] Information about the dielectric profile can be obtained by a fit of an assumed mathematical shape (such as the Fermi profile—a tanh function of z) to results of ellipsometric measurements.[36] Section IV below includes further discussion of this model.

The dielectric properties of the interfacial region may affect solvation and chemical reactions in a significant way. The free energy of solvation of polar or charged species increases as the dielectric constant of the medium decreases, resulting in a change in the reaction free energy and the activation free energy, and thus, in the equilibrium and rate of the reaction. The solvation free energy of a nonreactive solute at the interface region determines its concentration profile, which is an important ingredient in electrical double layer theories. A number of examples will be discussed in detail in sections IV and V.

D. Surface Roughness

Density fluctuations described in terms of thermally excited capillary waves give rise to an apparent surface roughness which may be correlated with the surface tension. Although this global roughness is an important characteristic of liquid interfaces, it has become increasingly clear in recent years that the local surface roughness, which is a microscopic dynamical aspect of the surface, is more relevant to an understanding of the behavior of solutes at interfaces. For example, using fluorescence depolarization experiments, Wirth and co-workers have shown that the reorientation dynamics and the lateral diffusion of acridine orange at several water/hydrocarbon interfaces do not correlate with the bulk viscosity of the bulk media or with the surface tension,[40,41] but are affected by the molecular shape of the solute and the roughness of the interface.

Potentially, more direct information about the local roughness of liquid surfaces can be obtained by the scattering of atoms and molecules from the free liquid surface. Experiments of this type have been recently carried out by Nathanson and co-workers.[119−122] In this case, the orientational distribution of the scattered atoms and molecules and their energy distributions provide the link to the local microscopic structure. Although Nathanson and co-workers were able to correlate the sticking probability to the thermodynamic enthalpy of solvation, there is evidence from

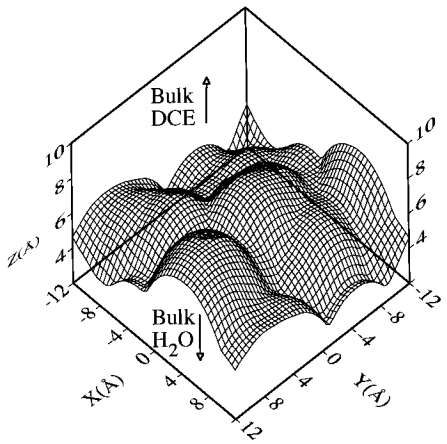

Figure 3. A snapshot of the water surface in contact with 1,2-dichloroethane. Shown is the Conolly surface of the water's oxygen using as a probe a ball of radius 5 Å. The Gibbs surface is at $Z = 4$ Å.

molecular dynamics simulations that surface roughness plays an important role in determining the orientational distribution and the initial fate of the colliding molecules.[123−125]

Perhaps the most important role of the local surface roughness may be realized in the case of the liquid/liquid interface. An example of the type of roughness encountered is shown in Figure 3, in which a snapshot of the water/DCE interface is represented using a Conolly surface plot.[126] The ability of reactant molecules to approach each other at the interface, when they are restricted to being in different phases, may be changed significantly if an appreciable roughening of the interface is possible. The transfer of solute across the interface may also be assisted by surface roughness. These topics will be discussed in more detail below.

To summarize this section, a number of the properties of the liquid interfacial region, such as the density, the viscosity, and the dielectric constant, have a bulk counterpart, and their effects on chemical reactions and solvation can be discussed, at least as a first step, in terms of concepts which have been developed for bulk phenomena. However, the interfacial region is also characterized by a number of properties that are qualitatively unique to the interface region, and their effect on chemical reactivity is less clear. This includes the structural and dynamical surface roughness, the specific molecular orientation, and other unique microscopic structural features. In the rest of the paper we will present examples to demonstrate all of the above liquid interface characteristics.

III. Isomerization Reactions

A. General Discussion

Isomerization reactions are some of the simplest and most common chemical processes. They have been used extensively to study solvent effects on the rate and equilibrium of bulk solution chemical reactions.[47,48,106,127−129] As a result, they represent a class of reactions in which solvent effects are relatively well understood, and thus they are an attractive choice for understanding solvent effects on interfacial chemical reactions. More importantly, in recent years, experimental data on the rate and equilibrium of interfacial isomerization reactions are beginning to be reported with the help of new experimental techniques.

Experimental studies of solvent effects on chemical reaction rates are sometimes difficult to interpret because the rate is affected by both equilibrium changes in the reaction free energy (which determines the transition state theory rate constant) and dynamical corrections due to the solvent friction.[47] One may get around this by assuming that one of the effects is small, or by considering a sequence of reactions where one effect stays approximately constant. By using molecular dynamics computer simulations,[48] it is possible to disentangle the static and dynamic effects and learn about the way in which the solvent environment influences the reaction at the microscopic level. This is the approach that is stressed below.

B. Experimental Observations

The first study of the rate of isomerization reactions at liquid interfaces was carried out by Sitzmann and Eisenthal.[15] They used picosecond SHG to measure the rate of the *cis*−*trans* interconversion of DODCI (3,3′-diethyloxodicarbocyanine iodide) at the water/air interface, and they compared it with the isomerization reaction in bulk water. They found that the reaction rate at the interface is about a factor of 2.5 larger relative to the rate in the bulk. Assuming that the activation energy for this reaction at the interface is equal to or greater than the one in the bulk (given the more polar nature of the transition state than the reactants), Sitzmann and Eisenthal have interpreted the effect on the rate as being due to the smaller friction at the interface.

Scott, Liu, and Doubleday[130] used picosecond multiple light scattering to study the photoisomerization of stilbene at the Al_2O_3/hexane interface. They found that this reaction is slower at the liquid/solid interface than in bulk hexane. It is likely that this effect is due to the adsorption at the solid surface and is not a "solvent effect". There are numerous studies of stilbene isomerization in bulk liquids.[131] Thus, an examination of this reaction in a variety of liquids with the same solid surface (and therefore, similar binding) may shed light on the interfacial liquid effects.

A similar case of isomerization at the liquid/solid interface was studied by Meech and Yoshihara.[18] They used picosecond SHG in a total reflection geometry to measure the rate of the photoisomerization of malachite green at the diethyl ether/quartz interface, as well as at the quartz/air interface. They found the rate of reaction at these two surfaces to be almost identical (and also similar to the rate at the silica/air interface[19]), but much slower than the reaction in the bulk liquid. Again, it seems that the adsorption on the solid surface is the main effect. However, it is known that the rate of this reaction is very sensitive to the viscosity of the bulk liquid.[46] Thus, studies of this reaction at the quartz/liquid interface with a variety of liquids would prove most interesting.

Obviously, much more experimental data are needed before a thorough understanding of interfacial solvent effects on simple isomerization reactions is gained. In particular, a systematic study of liquids of different viscosities is necessary. However, even at this point, several questions emerge from the experiments discussed above:

(1) Can one understand the effect of the interfacial region on the rate of reaction by considering the effective liquid density and viscosity at the interface, or are there unique surface effects that cannot be accounted for by simply assigning to the interface region a new effective density and viscosity?

(2) What is the relative importance of the equilibrium vs the dynamic solvent effect when one considers the change in the rate of the reaction from the bulk to the interface?

The theoretical models discussed below are preliminary attempts to shed light on these issues.

C. A Simple Model of an Interfacial Isomerization Reaction

The brief survey of available experimental data suggests that for isomerization reactions in simple nonpolar liquids, or in the case of reactions that do not involve significant change in the charge distribution, liquid interfacial effects result from the change in the solvent's density and viscosity. As discussed in section II.A, for a reaction that involves a change in the volume occupied by the reactants and products, the reduced density at the liquid/vapor interface will change the free energy of the reaction, and thus, the equilibrium constant. A similar consideration applies to the activation free energy, and thus, the transition-state theory rate constant. The reduced viscosity at the liquid/vapor interface may decrease or increase the rate relative to the value in the bulk liquid, depending on if the rate-limiting step is energy activation or diffusion across the barrier, respectively. At the solid/liquid interface, where the liquid density and viscosity is higher than that in the bulk, an opposite behavior is expected.

These simple considerations may be examined quantitatively by a simple model isomerization reaction that has been used in the past to study solvent density and viscosity effects in bulk liquids.[127,132] The reaction system consists of two atoms moving along the interatomic distance r between a compact and an extended state under the influence of the double-well potential:

$$U(r) = V_0[4((r - r_0)/R)^2 - 1]^2 \qquad (4)$$

where R is the distance between the two minima and r_0 is the location of the barrier whose height is V_0. This reaction is studied at the liquid/vapor interface of a 6−12 Lennard-Jones atomic liquid, and at the interface between a 6−12 Lennard-Jones liquid and a flat solid surface whose interaction with the liquid is modeled using a standard 9−3 Lennard-Jones potential. The center of mass of the diatomic is restricted to being near the Gibbs dividing surface in the case of the liquid/vapor interface, and physisorbed to the solid surface in the case of the liquid/solid interface. The reaction free-energy profile and the rate of the reaction have been calculated and compared with the results in the bulk Lennard-Jones liquid.

1. Equilibrium

Figure 4 presents a summary of the free-energy profile as a function of the reaction coordinate r for the different systems (we use reduced units: $r^* = r/\sigma$, where σ is the Lennard-Jones distance parameter). The symmetric double-well potential of the free diatom (the gas phase potential) is shown in the top solid line. It becomes asymmetric in the bulk liquid (bottom solid line), reflecting the negative free-energy contribution of the solvent at interatomic distances much smaller than typical interatomic distances in the pure liquid[133,134] (around $r^* = 1.1$ for a Lennard-Jones liquid in the liquid/vapor coexistence region). Thus, although the free energy of the extended state is almost unchanged, the compact state is stabilized by about $4kT$.

At the liquid/vapor interface, the lower density (about 50% of the bulk value) makes the solvent contribution to the free energy less negative by about a kT.[135] This is the expected effect, as discussed earlier. It can be semiquantitatively explained by a consideration of the dependence of the bulk liquid radial distribution function (or, more directly, the cavity distribution function) on the density.[134]

At the solid/liquid interface,[136] the free energy profile shows that the compact state is only slightly more stable than that at the liquid/vapor interface, which would seem to be consistent with the higher density of the liquid. However, the reaction free energy profile also includes a contribution due to the adsorption on the solid surface. Since this contribution can be independently calculated,[136] to be $2kT$, one in fact finds that the solvent contribution at the solid/liquid interface is less negative than even that at the liquid/vapor interface, despite the fact that the density of the liquid near the wall in the system considered in Figure 4 is about 3 times the bulk density![136] This result can be explained by realizing that when the diatomic solute is adsorbed at the surface, not all of the solvent molecules are available

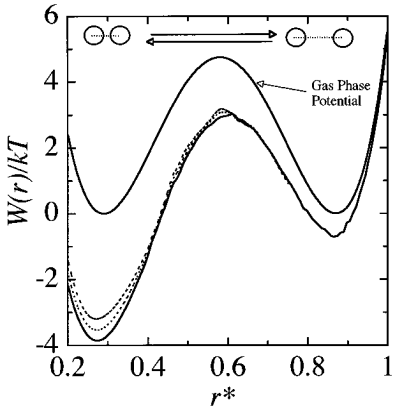

Figure 4. The reaction free energy for an isomerizing diatomic in the gas phase (top solid line), in the bulk of a Lennard-Jones liquid (bottom solid line), at the Leonard-Jones liquid/solid interface (bottom dotted line), and at the Lennard-Jones liquid/vapor interface (top dotted line). In all cases, $T^* = 0.9$. (Taken from ref 172. Copyright 1995 American Chemical Society.)

to solvate it. Thus, although the effective density is high, a significant portion of the space around the diatomic solute does not include any solvent molecules. This is expected to be even more pronounced when the reactants are more strongly adsorbed to the solid surface.

The reaction free energy profile can be used to estimate the effect of the interface on the transition-state theory rate constant. Specifically, at both the liquid/vapor and the liquid/solid interface, the compact state is destabilized compared with that in the bulk, whereas the transition state is unaffected (compare the three lower curves in Figure 4). Thus, for the model discussed here, the transition-state theory rate constant will be higher by about a factor of 2. The correct rate constant includes dynamical solvent effects, which will be considered next.

2. Dynamics

Studies of the model reaction system discussed above in bulk liquids at densities close to the one considered here show[132] that the rate constant for the isomerization reaction diminishes as the density increases, due to an increase in the recrossings of the transition state. Even though the system reaches the transition state with the correct velocity (toward the product), it may reverse direction and not react. This is quantitatively reflected by the probability of crossing, or transmission coefficient κ, being less than one. Typical values of κ are between 1 and 0.1, and thus are not that important in correcting the absolute rate constant. However, we have just noted that typical equilibrium surface effects can be of the same order and thus it is important to investigate what the dynamic solvent effects would be at liquid interfaces.

The lower viscosity and density at the liquid/vapor interface suggest that the number of recrossings will decrease, κ will be closer to one, and the rate constant will increase relative to the bulk, other things being unchanged. This is indeed what has been found in molecular dynamics calculation of κ. At the liquid/solid interface, a very mild increase in κ has been observed, despite the increase in the apparent viscosity of the liquid.[136] These calculations are performed by initiating trajectories at the transition state in the direction toward the product state and then counting the trajectories that were able to continue to the product-state well.[48]

The exact value of κ depends on the reaction free-energy profile, in particular the barrier frequency. In order to better understand the above results, one may calculate the friction exerted by the solvent on the reaction coordinate, which is approximately independent of the shape of the reaction system potential. The dynamic friction on the reaction coordinate is calculated using:[47,106,137]

$$\zeta(t) = \beta/\mu\langle f(t)f(0)\rangle_c \qquad (5)$$

where $\beta = 1/kT$, μ is the reduced mass of the diatomic solute and $f(t)$ is half the total force along the diatom bond at time t. The subscript "c" refers to the "clamping approximation", where the force is calculated while the bond distance is fixed at the transition state.[47,106,137]

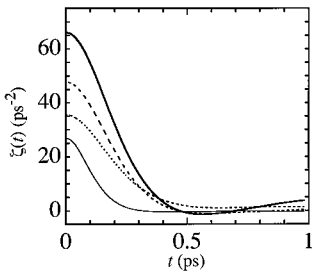

Figure 5. The time-dependent friction on the reaction coordinate for an isomerizing diatomic in various environments: solid line, in the bulk Lennard-Jones liquid ($T^* = 1.0$, $\rho^* = 0.78$); dashed and dotted lines, the diatom is adsorbed at the liquid/solid interface with fixed parallel and perpendicular orientation, respectively (same T and ρ); thin solid line, at the liquid/vapor interface ($T^* = 0.9$, $\rho^* = 0.74$).

Figure 5 shows the dynamical friction on the reaction coordinate in the bulk liquid (solid thick line), at the liquid/vapor interface (thin solid line) and at two different fixed orientations at the liquid/solid interface. The shape of the curve is very similar in all cases, the main difference being the value of the zero-time friction. At the liquid/vapor interface, the reduced density causes less frequent collisions with the diatomic solute, and less friction. At the liquid/solid interface, the force along the reaction coordinate due to the collisions with the liquid atoms depends on the orientation of the diatom. When it is perpendicular to the interface, the atom closer to the wall is almost unable to experience collisions with a significant component along the bond, and the friction in this case is smaller than in the case where the diatom is parallel to the interface. In both cases, the friction is less than in the bulk because of the less frequent collisions with the liquid atoms when the diatomic molecule is adsorbed on the solid surface.

Knowledge of the dynamic friction $\zeta(t)$ allows for an approximate calculation of the transmission coefficient for different reaction profiles,[47,106,137,138] thus avoiding the need for a full molecular dynamics calculation of the transmission coefficient. For details about these calculations, the reader is referred to the original papers.[135,136]

Although the simple model discussed above is an extremely simplified representation of the real experiment, it is worthwhile noting that at the liquid/vapor interface, one indeed gets an enhancement of the rate due to a transmission coefficient being closer to 1 than in the bulk liquid. At the liquid/solid interface, the dynamical solvent effect also leads to a slight increase in the rate, contrary to the observation of a slower rate at the surface. This suggests that the main effect in the experimental system is a strong adsorption of the solute to the solid surface. Indeed, as the analytical calculation of the surface contribution to the reaction profile shows,[136] by increasing the well-depth of the solute/surface 3−9 Lennard-Jones potential, the activation energy can be made significantly larger than the one in the bulk liquid. Finally, it is interesting to note that in both liquid interfaces discussed above, the magnitude of the equilibrium interfacial solvent effect is comparable to the magnitude of the dynamic effect, a result

that may have wider applicability in cases of weakly adsorbed reactants.

D. Isomerization Reactions at Aqueous Interfaces

Isomerization reactions in polar solvents that involve a change in the molecular dipole moment as the conformation changes, may exhibit much more dramatic interfacial effects because the lower effective dielectric constant at the interface may significantly alter the reaction free-energy profile. As in the previous model, an investigation of solvent effects on the rate requires consideration of both equilibrium and dynamic effects.

1. Gauche–Trans Isomerization at the Water Liquid/Vapor Interface

A study of the *gauche−trans* isomerization reaction of 1,2-dichloroethane (DCE) at the water liquid/vapor interface has been reported by Benjamin and Pohorille.[139] In this case, the reaction coordinate is the Cl−C−C−Cl torsional angle ϕ. In the *gauche* state ($\phi \approx 60°, 300°$), the molecule has an appreciable dipole moment of 3.2 D, whereas in the *trans* state ($\phi \approx 180°$), the total dipole moment is near zero. Studies of the torsional free-energy profile of this molecule (the potential of mean force) in bulk polar liquids, using integral equation theory[140] and molecular dynamics computer simulations,[141−144] demonstrate that the *gauche−trans* population ratio increases in polar solvents compared with the ratio in the gas phase, due to the stabilization of the more polar *gauche* conformer. Thus, one expects to see a decrease in this ratio at the water liquid/vapor interface relative to the ratio in bulk water.

The calculations of the free-energy profile were performed on a system that included 343 TIP4P water molecules and one DCE molecule at the liquid/vapor interface of the water slab at $T = 300$ K. The DCE was modeled using an all-atom fully flexible potential. To increase the accuracy of the calculations and their sensitivity to the solvent effect, the free energy calculations were done using a biasing potential that allows for a uniform sampling of the reaction coordinate.[139,145] The results (in terms of populations) are shown in Figure 6.

The fractional population of the *gauche* conformer, obtained by integrating the two peaks at 60° and 300°, changes from 0.23 in the gas phase (the experimental value is 0.21[146]) to 0.73 in bulk water. This result is consistent with the fractions 0.65 and 0.47 calculated in pure DCE[141] and in methyl chloride,[143] respectively, which are less polar than water. At the water liquid/vapor interface, the *gauche* fraction is 0.5, falling between the gas phase and the bulk water fractions, and clearly in agreement with the qualitative argument presented earlier: There is a destabilization of the more polar conformer at the water surface.

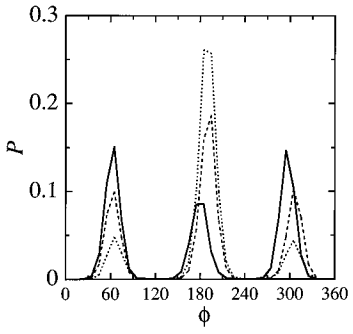

Figure 6. The probability distribution function for the torsional angle in a single 1,2-dichloroethane molecule in bulk water (solid line), at the water liquid/vapor interface (dashed line) and in the gas phase (dotted line). In all cases, $T = 300$ K. (Taken from ref 139. Copyright American Institute of Physics.)

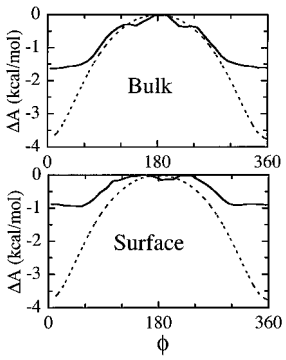

Figure 7. The solvent contribution to the torsional potential of mean force for a single 1,2-dichloroethane molecule in bulk water and at the water liquid/vapor interface: solid lines, molecular dynamics free energy calculations; dashed lines, a continuum electrostatic model. (Taken from ref 139. Copyright American Institute of Physics.)

In order to be a bit more quantitative about the surface effect, one can compute the solvent contribution to the potential of mean force by using the populations in Figure 6. The results of the solvent contribution in bulk water and at the surface are shown in Figure 7. The water contribution to the stabilization of the *gauche* conformer relative to the *trans* conformer is −1.4 kcal/mol in bulk water and −0.7 kcal/mol at the surface. Figure 7 also shows the result of a continuum dielectric calculation of this quantity. The computation involves the free energy required to "charge up" a DCE molecule (represented by four point charges imbedded in spherical cavities) at a sharp dielectric model of the water surface.[74] Although the general trend of stabilizing the more polar conformer is reproduced, the surface effect is essentially nonexistent (in both cases, the solvent contribution is −2 kcal/mol), in addition to the overestimation of the stabilization of the more polar conformer. It is possible to recover the surface effect by allowing the hard spheres (which represent the DCE atoms) to cross the sharp interface. However, this will result in a worse overestimation of the difference between the *gauche* and *trans* free energy. A more detailed examination of the continuum electrostatic model will be presented later.

As in the model discussed in the previous section, the effect of the interface on the rate constant for the *gauche* → *trans* isomerization reaction includes equilibrium and dynamical contributions. Figure 6 shows that the activation energy for this reaction at the water surface is 0.4 kcal/mol smaller than in the bulk. This corresponds to an increase in the rate by a factor of almost 2. The main reason for this is that the *gauche* form is destabilized at the interface relative

to the bulk, but the transition state (at $\phi \approx 120°$), which is much less polar, is almost unaffected by the transfer to the water surface. To complete the discussion, one must determine the fraction of trajectories that cross the transition state. In this case, one finds[139] that although κ may be as low as 0.6, the values in the bulk and at the interface are almost the same. Nevertheless, the dynamical behavior of the trajectories is quite interesting, and the reader may consult the original paper for details.

2. Gauche–Trans Isomerization at the Water/Organic Phase Interface

Although no experimental data are available about the rate and equilibria of isomerization reactions at the liquid/liquid interface, there are important problems in cellular biology for which an understanding of the equilibrium and dynamics of flexible molecules could be relevant. For example, the rate of transport of neurotransmitters, anesthetics, antibiotics, and other drugs across the water/membrane interface may depend on their conformational state. The time scale for the conformational transitions compared with the surface residence time for each conformer will determine the mechanism of the transfer. The problem is complicated because it involves calculations of the torsional potential of mean force as a function of the distance along the interface normal.

A detailed study of these free-energy surfaces, the conformational dynamics as well as the transfer rate across the liquid/liquid interface was carried out by Pohorille and Wilson for 1,2-dichloroethane (DCE) and an alanine dipeptide at the water/hexane interface.[147] The free energy of the *gauche* and *trans* conformers of DCE as a function of the distance from the interface, as well as the torsional potential of mean force, were computed. The rate of the *gauche* → *trans* isomerization reaction at the interface was found to be much faster than the surface residence time of each conformer. Thus, the transfer is controlled by the escape rate from the local free-energy minimum at the interface. For the alanine dipeptide, there are different stable conformational states in water and in hexane. The barrier between them is reduced at the interface, and the molecule adopts an orientation which allows for the polar group's maximum contact with water, while the nonpolar group is buried in the hexane. The conformational equilibrium is rapidly established in this case, as in the case of DCE.

IV. Solvation at Liquid Interfaces

In the previous section, we discussed the fact that an important step in understanding liquid interfacial effects on chemical reaction equilibrium and rate is determining the change in the solvation free energy of the reactants, products, and the transition state. We devote this section to a more thorough discussion of this important aspect of understanding interfacial chemical reactivity. Because most of the systems studied involve the solvation of charged and polar solute at aqueous interfaces, in this section we will discuss the solvation of ions and polar solutes at the water liquid/vapor interface. The solvation of ions at the liquid/liquid interface is an integral part of the problem of the ion-transfer process, and it will be discussed in section V.B. Solvation at the metal/water interface has been extensively reviewed recently,[54,117] and only a brief survey of recent results will be discussed in section IV.B.3 below.

A. Overview and Experimental Background

An important problem in physical chemistry is the understanding of solvation at the thermodynamic and microscopic levels.[148,149] In the last few years, significant progress in experiments and theory have presented an intriguing new picture of solvent effects,[150−155] which complements the large body of knowledge gained since the beginning of the century using thermodynamic and continuum level approaches. This progress has been an integral part of our current understanding of solution phase physical chemistry. Unfortunately, much less is known about solvation at liquid interfaces, and most of what is known is mainly limited to some indirect experimental data, such as the surface potential and surface tension of ionic solutions and a macroscopic continuum level description.[55]

The development of nonlinear optical techniques is beginning to provide a wealth of new data about the behavior of solutes at liquid interfaces. The basic idea of these experiments is that within the electric dipole approximation, the second-harmonic response of a system is generated mainly by molecules that reside at the interface. The magnitude and polarization dependence of the signal give information about the number of these molecules and their orientation.[8,11] This technique has been used to study the adsorption of solutes at the liquid/vapor, liquid/liquid and liquid/solid interfaces, in addition to earlier work on the solid/vacuum interface. A survey of many of these experimental results has recently been presented by Eisenthal[9] and by Corn and Higgins.[11]

With recent advances in the study of chemical reaction dynamics and equilibrium at liquid interfaces, it has become clear that a better understanding of solvation in these environments, especially at the microscopic level, is necessary. A few examples clearly demonstrate this: Using SHG, Bhattachryya *et al.* found that the equilibrium constant for the acid dissociation of *p*-nitrophenol at the air/water interface is shifted toward the neutral molecules by a factor of 50−100.[16] Obviously, a quantitative explanation of this shift must involve a computation of the free-energy of ion solvation at the water surface. Similarly, Xiao *et al.*[156] have observed dramatic changes in the SHG signal upon the protonation of the acid−base groups of monolayers adsorbed at the air/water interface. Studies of other reactions[9,15,26] and of the adsorption of ionic and neutral solute at water surfaces[10,14,20,21,157−162] depend for their interpretation on a quantitative understanding of solvation at the water surface. Another example is the uptake of SO_2 by water droplets, studied by Davidovitz, Worsnop, and co-workers.[163] The uptake rate was found to be faster than expected on the basis of the reaction rate between this gas and water in the bulk. However, it is clear that the interfacial solvation of the HSO_3^- ion must be an important factor

in affecting the rate of this reaction. A number of charge transfer reactions at the liquid/liquid interface, whose interpretation depends on understanding the behavior of ions at the liquid/liquid interface, have been recently studied. This topic will be discussed separately in section V.B below.

A molecular level understanding of solvation at liquid interfaces is important for the correct interpretation of the above and other, interfacial phenomena. This is one aspect that will be discussed below. However, another important goal of these studies has been to understand the limitations of continuum models in providing a quantitatively accurate picture of interfacial solvation. Both the thermodynamic, static aspect of solvation and the dynamics of solvent reorganization will be considered below.

The simplest possible problem of interfacial solvation is that of a solute at infinite dilution at the water liquid/vapor or liquid/solid interface. In this case, one can avoid the complicated issues of finite ionic concentration, double-layer effects, and interionic interactions, which make a full microscopic description of the inhomogeneous system intractable. These issues have been discussed by many workers and have been recently extensively reviewed,[52,164−167] and thus they will not be considered here except to provide some relevant information.

Even the simple problem of a single solute at a water surface is too demanding for a statistical mechanical treatment which includes a microscopic solvent description. Thus, this problem has been studied using continuum models and computer simulations, and it will be discussed next.

B. Equilibrium Solvation at Liquid Interfaces

1. Preliminaries

The solvation free energy of ions and other solutes in bulk solvents can be determined by standard free-energy simulation techniques,[57] for example, by calculating the reversible work necessary to "grow" the solute from nothing to its final size and charge. This gives the absolute free energy of solvation, which is quite sensitive to the choice of potentials and boundary conditions. At the planar water surface, the solvation free energy will depend on the location of the solute along the interface normal, which further complicates things. However, if one is interested in the solvation free energy relative to the value in the bulk, the resulting free energy profile is much less sensitive to the choice of potentials and boundary conditions, and it is, in fact, more relevant to the issue of interfacial solvent effects on chemical reactivity.

If $P(z)$ is the solute position probability distribution function, then the free energy profile is given by[50,53]

$$A(z) = -\beta^{-1} \ln P(z) = -\beta^{-1} \ln\langle\delta(z_S - z)\rangle \quad (6)$$

where $\beta = 1/kT$, δ is the Dirac δ function, z_S is the location of the solute along the interface normal and the ensemble average is over the position of all particles (the liquid and solute). In the bulk region, $A(z)$ is independent of z because of translational invariance. We take it as our zero free energy point.

Despite its apparent simplicity, there are no statistical mechanical (analytical or numerical) calculations of it for a solute at the liquid/vapor interface of water (or any other model liquid). One problem is that the integral in eq 6 involves an interfacial liquid pair correlation function, which is very difficult to compute, even for simple inhomogeneous liquids.[52] Thus, all of our current knowledge about the free-energy profile $A(z)$ has been obtained through simulations. These simulations involve the use of a biasing potential which allows for an adequate sampling of the high free energy region.[168] The particulars about the choice of the biasing potential and other technical details can be found elsewhere.[169−171]

We review here some results on free-energy profiles of a solute at the liquid/vapor interface of water and the water/metal interface. Results on the liquid/liquid interface will be discussed in section V.B, on ion transfer across the interface.

2. Ion Solvation at the Water Liquid/Vapor Interface

Figure 8 shows the results of such a calculation for a chloride ion at the water liquid/vapor interface.[172] The system includes 343 water molecules modeled using a flexible SPC potential,[171] and a single chloride ion interacting with the water via a Lennard-Jones plus coulomb potential. The calculations were also done for a chloride ion whose charge was reversed ("Cl^+"). As the figure shows, there is a significant free-energy increase as the ions move toward the interface. This is, of course, consistent with the common knowledge (based on surface tension measurements of dilute electrolyte solutions) that small ions are "repelled" from the interface.[55] The free energy of adsorption may be taken to be $A(z_{Gibbs}) - A(z_{bulk})$, which is around 10 kcal/mol. This suggests that there is an ion-free region of few angstroms near the Gibbs surface. The free energy profile also show that the ions begin to "feel the surface" when they are about 8 Å away from the Gibbs surface, even though the water structure at this distance is nearly indistinguishable from the structure of bulk water (according to simulations).

The free energy profile of "Cl^+" shows that this positive ion begins to feel the interface when it is

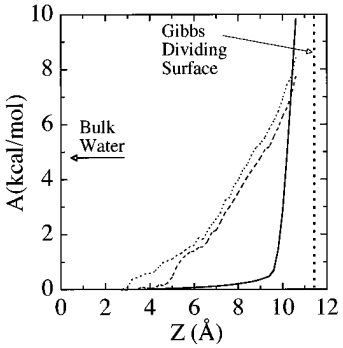

Figure 8. The adsorption free energy of an ion as a function of the distance along the normal to the water/liquid vapor interface at $T = 300$ K; solid line, a continuum electrostatic model calculation based on a sharp interface located at the Gibbs surface (11.5 Å from the center of the lamella); dashed line, molecular dynamics free energy calculations for Cl^-; dotted line, molecular dynamics calculations for "Cl^+" (see text). (Taken from reference 172. Copyright 1995 American Chemical Society.)

further away than the negative ion. This result is consistent with surface potential measurements[173] and thermodynamic models based on the Gibbs isotherm equation and surface tension, which suggest a lower concentration of positive ions than negative ions of approximately the same size. A detailed analysis of the structure of water as the ion is being pulled toward the interface has been carried out by Wilson and Pohorille.[170] By considering the orientation of water dipoles, they found greater resistance to driving positive than negative ions toward the interface. When an ion is pulled beyond the Gibbs surface, a significant "bulge" develops in the water, which suggests that the ion tends to keep its solvation shell. This point has also been addressed by Benjamin,[171] who found that the contribution of the first shell to the ion interaction energy is mildly affected by the transfer to the surface. We will see later that this is a general result for ion at interfaces, and it has important consequences for solvation dynamics and charge-transfer reactions.

In addition to providing some microscopic detail that is very valuable (and almost impossible to gain by any other means), the simulation results of ionic solvation can be used to test the only other approximate theoretical treatment of ion adsorption free energy at interfaces—the continuum electrostatic model. In the simplest form of this model, the ion is represented by a spherical charged cavity, and the interface is the mathematically sharp border between two dielectric slabs whose dielectric constants are taken to be equal to 1 (vacuum) and 82.5 for bulk water (flexible SPC model). The free energy of charging this ion is numerically calculated by solving the Poisson equation. It is assumed that other contributions to the solvation free energy (mainly the cost to create the cavity) do not vary appreciably as the ion approaches the interface.

The solid line in Figure 8 shows the result of this calculation. The cavity radius (2.3 Å) is taken to be the value which reproduces the solvation free energy of the chloride ion in bulk SPC water, and the interface location is taken to be the Gibbs dividing surface. The continuum model underestimates the free energy a few molecular diameters "below" the interface, and overestimates it when the cavity begins to cross the interface. It is easy to show that this will be the case for other choices of the interface location.

Another possible continuum model is the one based on the dielectric profile $\epsilon(z)$. On the bulk side of the Gibbs surface, this model will have an effective dielectric constant which is smaller than that of bulk water, and on the vapor side of the surface it will have a value which is greater than 1. Consequently, the free energy curve will look more like the molecular dynamics results. In fact, one does not need to calculate the solvation free energy of a finite size cavity in such a medium to realize that it is possible to find a profile that will exactly match the molecular dynamics results. Does this mean that the continuum model with a dielectric profile is a fair representation of the solvation of a simple ion at the interface? We will see below in section C that, in fact, this model is a poor choice as far as the solvation dynamics are concerned.

3. Ionic Solvation at the Water/Metal Interface

The solvation of ions and molecules at the water/metal interface is one aspect of the more general problem of the structure of the electrolyte/electrode interface. This subject is discussed at length in every textbook on electrochemistry,[2] with the focus being on treating the solute and the metal with great care and, typically, on assuming a simple continuum model description of the solvent. In recent years, due to advances in *in situ* experimental techniques[45] and in the theoretical understanding of the molecular structure of water at the metal surface,[52,174] there has been an effort to treat all aspects of the problem at the microscopic level.[167] In this section, we briefly review the progress of treating ionic hydration at a metal electrode using a full microscopic water model. For treatment of the same problem using a simplified water model see ref 52.

The first attempt to study the ionic distribution profile at the water/solid interface was by Spohr and Heinzinger, who studied a system of $8Li^+$ and $8I^-$ ions dissolved in 200 water molecules between uncharged flat Lennard-Jones walls.[80] However, the question of ionic hydration was not addressed.

Rose and Benjamin[175] considered in detail the structure of the hydration shell around Na^+ and Cl^- ions at the water/Pt(100) interface, and they determined the free energy profile for the adsorption of these ions. The water−Pt potentials developed by Spohr and Heinzinger were used.[81,82,115] In addition, a form of ion−metal image interactions was included. They found that although the structure of water at the interface is significantly different from the structure in the bulk, the structure of the hydration complex is relatively unperturbed. The free energy profile is nonmonotonic and shows a barrier to adsorption. The different behavior of the negative and positive ions mirrors the behavior at the water liquid/vapor interface discussed above. In a later study, the effect of charges on the metal was investigated.[176] Unless the external electric field is very high, the ions still keep their solvation shell. The electric field was also found to decrease the residence time of water molecules in the ion's hydration shell.

Seitz-Beywl *et al.*[177] studied the hydration shell structure of Li^+ and I^- at the interface between water and an uncharged Pt surface. They found that the ion size plays an important role in the ability of the ion to lose part of its hydration shell upon adsorption.

Glosli and Philpott[178] presented a systematic study of ion size effect, showing that although F^- and Cl^- keep their solvation shell, Br^- loses part of the shell and I^- is adsorbed with no water molecules interposed between the ion and the metal at any time. A similar stability of the Na^+ hydration shell upon adsorption was found by Matsui and Jorgensen[179] using a Monte Carlo simulation, which included ion−wall and water−wall image interactions.

Berkowitz and co-workers have developed an analytical representation of the atomic Pt/water interface[88] based on the Spohr−Heinzinger potentials. They have used it to study the adsorption of Li^+ and

I^- at this interface.[180] In agreement with previous studies, they have found that the I^- anion contact adsorbs, with no water molecules between the anion and the surface. However, even though the Li^+ adsorbs with a full hydration shell, it is much closer to the metal surface than one might expect based on the ion-free Helmholtz layer concept.[181] They also computed the free-energy profile and found that the barrier to adsorption for Li^+ is greater than that of I^-.

An important conclusion of many of the above studies is that although the water structure near the metal is significantly different from that of bulk water, the strong water−ion interactions are able to compete with the structural constraints imposed by the surface on the interfacial water molecules, and to leave the hydration shell of small ions intact. We will see later that this has important implications for electron-transfer reactions.

4. Solvation of Other Solutes at Liquid Interfaces

Although the results of the molecular dynamics simulation of the adsorption of small ions are consistent with the indirect experimental data on the adsorption of these ions, a more direct comparison with experimental data would be desirable. This has been recently possible thanks to a wealth of optical SHG results provided by several workers.[9,11] Because the optical second-harmonic signal is produced by the optical transition of the valence electrons, the signal is particularly easy to detect from molecules with an extended π−orbital system. These molecules are quite large, and thus, the contribution to the solvation free energy due to the hydrophobic nature of the solute needs to be considered in addition to any electrostatic contributions.

In a series of experiments by Eisenthal and coworkers, the competition between the hydrophobic and electrostatic effects in determining the adsorption and solvation of solute molecules at the water liquid/vapor interface was clearly demonstrated.[14,20,21] In these experiments, the adsorption isotherm of a series of alkylphenol $CH_3(CH_2)_nC_6H_4OH$ and alkylaniline (the OH is replaced by an NH_2 group) was determined by monitoring the SHG signal as a function of bulk concentration. From this data, the adsorption free energy for molecules with varying alkyl chain lengths was determined. Phenol and alkylphenol are surface active—their hydrophobicity is reflected in their tendency to adsorb at the water liquid/vapor interface—and so, unlike the small ions discussed earlier, the transfer to the interface involves a lowering the solvation free energy. However, when the phenol is deprotonated to produce the phenolate anion (which is controlled by the bulk pH), the molecule surface activity is lost and the minimum free energy is in bulk water. By increasing the length of the alkyl chain one can reach the point where the molecule again becomes surface active. Of course, all of this has been well known for many years from simple surface tension measurements,[7,182] but what these recent experiments were able to provide is accurate information about the surface concentration and the ability to determine the precise balance between the electrostatic and hydrophobic driving forces. In particular, it was found that each CH_2 group lowers the adsorption free energy by 0.78 kcal/mol, and five such groups are required to restore the surface activity of the phenolate anion.

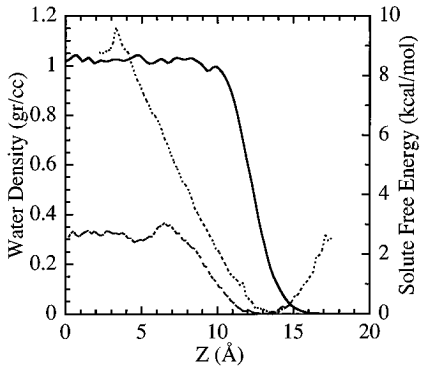

Figure 9. Adsorption free energy profile for phenol (dashed line) and for pentyl phenol (dotted line) at the water surface ($T = 300$ K). Also shown is the density profile of water (solid line). $Z = 0$ is the center of the water lamela. The Z position of phenol is its center of mass, and for pentyl phenol it is the position of the para carbon (also close to the center of mass).

In an effort to understand the microscopic structural changes involved in the adsorption of a surface active group, and in particular, how the competition between the hydrophobicity of the hydrocarbon chain and the hydrophilicity of the polar group determines energetics and molecular orientation, Pohorille and Benjamin studied the adsorption of phenol[183] and pentyl phenol[184] at the water (TIP4P model) liquid/vapor interface using molecular dynamics computer simulations. The results of the free-energy profile for these two molecules are shown in Figure 9. Unlike the profiles shown in Figure 8, the curves are nonmonotonic. The free energy minima are at the interface region, on the vapor side of the Gibbs surface. The adsorption free energies are -2.8 ± 4.0 and -8.8 ± 0.7 kcal/mol for phenol and pentylphenol, respectively, in reasonable agreement with the experimental values of -3.8 and -7.3 kcal/mol, respectively. Note also the small barrier located in the bulk water (9 and 6 Å away from the Gibbs surface for pentyl phenol and phenol, respectively). The location of these barriers corresponds to the point where the respective molecules begin to be rotationally constrained. Support for the existence of such barriers is provided by measurement of the adsorption rate, which is found to be slower than the diffusion time.[20] Other structural information such as the molecular orientation (the OH group points toward the bulk water, as expected and in agreement with the experiments) and conformations of the pentyl phenol can be found in the original papers.[183,184]

C. Solvation Dynamics at Liquid Interfaces

In recent years, it has become increasingly evident that in cases of fast charge-transfer reactions in polar liquids, the energetics and structural characteristics of the equilibrium solvation may not be realized in the short time scale of these reactions. One needs to consider the situation where the solvent dipoles are out of equilibrium with the charged solute, and to understand that this situation has significant

implications for the rate of reactions.[151−154,185−194] With the application of time-resolved, nonlinear optical techniques to the study of charge-transfer reactions at interfaces, the issue of nonequilibrium solvation and the dynamics of the relaxation toward equilibrium solvation will have to be critically examined for interfacial reactions as well. This will be further considered in section V below. In this section, we use the solvent dynamical response to a newly created charge distribution to provide an additional check on the continuum electrostatic model of small ion solvation presented earlier in section IV.B.2. In that section, it was shown that a continuum electrostatic model with a sharp boundary between the liquid and the vapor phase does not provide an accurate representation of the free-energy profile of ion adsorption and that an inhomogeneous dielectric model is required to obtain agreement with the molecular dynamics calculations. We consider now the ability of these two continuum models to describe correctly the dynamical response of the medium to a sudden creation of a new charge by comparing the results of these two models to a molecular dynamics simulation of interfacial solvation dynamics.

The response of a polar medium to a new charge distribution can be experimentally detected by following the time-dependent shift of the peak of the emission spectrum from a photochemically excited solute.[151,154] Theoretically, this process has been investigated by continuum electrostatic models,[185,195] molecular theories,[152,187−189] and computer simulations[192−194,196−198] by considering the correlation function

$$C(t) = \frac{\overline{U(t)} - \overline{U(\infty)}}{\overline{U(0)} - \overline{U(\infty)}} \qquad (7)$$

where $\overline{U(t)}$ is the ensemble average of the total electrostatic potential induced at the location of the solute at time t. This formula can be directly used to study the solvation dynamics in computer simulation. Starting from an equilibrium ensemble, the charge on the ion is changed and the potential is monitored. This is repeated for each member of the ensemble, and the averages are calculated. In Figure 10, we show in thin solid line and in dashed line the results of this calculation in bulk water and at the water liquid/vapor interface. It is clear that the response is almost identical! In both cases there is a very rapid initial decay, that represents inertial solvent motion,[192,199] followed by a nearly exponential decay. Before examining the microscopic reason for this result, we discuss the prediction of two continuum models. In comparing the molecular dynamics results to these models, we must only consider the long-time tail of $C(t)$, as the inertial response is not included in these models.

A particularly simple model calculation for $C(t)$ is based on the Debye continuum solvent model and predicts that the relaxation is exponential:

$$C(t) = e^{-t/\tau_L} \qquad \tau_L = \epsilon_\infty \tau_D / \epsilon_0 \qquad (8)$$

where τ_D is the Debye relaxation time, which is a measure of the time it takes for the polarization of a macroscopic sample of liquid to decay to zero after the electric field has been turned off, ϵ_0 and ϵ_∞ are the static and the infinite dielectric constant of the liquid, and τ_L is called the longitudinal relaxation time. A number of studies have found that although this model is not very accurate, it does provide a reasonable picture of the relaxation that can be improved by considering the finite size and mass of the liquid molecules.[152,187−189] We will use this model here to estimate the interfacial solvent response.

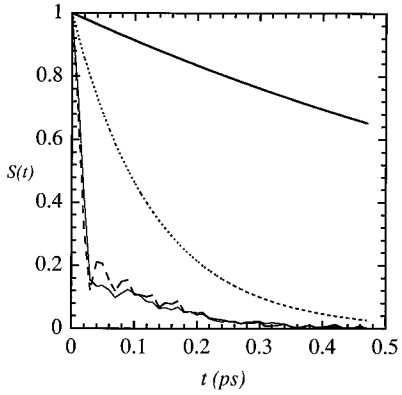

Figure 10. Water relaxation function following a charge neutralization reaction in the bulk and at the water liquid/vapor interface: dashed line, molecular dynamics in the bulk; thin solid line, molecular dynamics at the interface; dotted line, Debye continuum model in the bulk; thick solid line, Debye continuum model for the inhomogeneous interface model.

First we note that for bulk flexible SPC water at $T = 300$ K, $\epsilon_0 = 82.5$, $\epsilon_\infty = 1$, and $\tau_D = 11$ ps, which gives $\tau_L = 0.13$ ps. This is about a factor of 2 faster than the molecular dynamics results in the bulk, a reasonable agreement considering the simplicity of the model. The relaxation curve with this time constant is shown in Figure 10 as the dotted line.

Consider now the two different continuum models at the interface. From the dipole reorientation time at the water liquid/vapor interface we estimate $\tau_D = 9$ ps. Thus, for the sharp continuum model (with the ion in the bulk liquid side), the Debye model gives essentially the same result as in the bulk. This is because the dielectric constant is still 82.5, and the correction due to image effects can be shown to be negligible.[200] On the other hand, in the inhomogeneous dielectric model, the effective dielectric constant at the location of the ion is about 10, a value which reproduces the equilibrium free energy. This model gives a relaxation time that is about 1 order of magnitude slower than the molecular dynamics results (thick solid line in Figure 10). This discrepancy does not disappear if one takes into account finite solvent size. It serves to highlight a basic problem with the continuum model.

An examination of the contribution to the relaxation dynamics and to the energetics from different solvent shells in the bulk and at the interface, as well as an examination of the structure of the solvation complex,[171] show that the bulk and surface data are very similar. The ion tends to keep its solvation shell intact, and this results in a similar dynamic response since this response is mainly determined by the first solvation shell. Thus, one gets reasonable agreement with the sharp dielectric model but poor agreement

with the inhomogeneous dielectric model. In contrast, the solvation free energy involves contributions from all of the configuration space. This can be accounted for by the inhomogeneous model, but it is poorly described by the sharp continuum model. One way to improve this situation is to incorporate into the inhomogeneous dielectric model the fact that the first solvation shell of the ion is the same as in the bulk. This stability of the first solvation shell as the ion approaches the interface will be shown below to play an important role in many other systems.

Although we have used a very simple model for the dynamical response, and improvements are certainly possible, the above discussion suggests that care must be exercised in routine application of models that are found to be reasonable for bulk solvation when considering equilibrium and dynamic solvation at liquid interfaces.

V. Interfacial Charge Transfer Reactions

A. Overview

Charge transfer reactions at liquid interfaces are of basic importance in many areas. Examples include phase-transfer catalysis[3] at the water/organic phase interface, electrochemical liquid/liquid systems,[201] photoelectrochemical cells,[202] corrosions, and more. Until recently, most of our knowledge about the fundamental factors that govern charge-transfer reactions at liquid interfaces was based on macroscopic thermodynamics approaches.[7] This knowledge has been enhanced in recent years thanks to new experimental[11,45] and theoretical developments.[44,52,172] The purpose of this section is to consider the new microscopic level information about electron transfer and ion transfer at the liquid/liquid and liquid/metal interfaces. To keep the review to a reasonable size, we focus only on the issues that demonstrate the unique contribution of the interfacial region at the microscopic level. There are a number of reviews on the general aspects of charge transfer at interfaces[6,201] and on new developments in electron-transfer reactions[203] that should be consulted for a more general perspective.

B. Ion Transfer across the Interface between Two Immiscible Liquids

1. Preliminaries

Ion transfer across the interface between two liquids is found in many chemical processes, as for example in phase transfer catalysis,[3] where the reactants must cross the interface to initiate or complete a reaction at the interface between water and an organic phase. Other examples includes drug delivery problems in pharmacology[4] and electrochemical charge-transfer processes.[201] Thus, it is not surprising that the process of ion transfer has been extensively studied using a variety of experimental[204−215] and theoretical techniques.[201,216−221] Despite this effort, the mechanism of ion transfer across the interface between two immiscible liquids is not well understood. The fundamental reason is that very little is known about the microscopic structure of the interface, and almost all of the experimental data are not at a sufficient level of detail to allow for an unambiguous test of the different models. Some of the fundamental issues that are not fully resolved include: What are the molecular factors that influence the rate of the transfer? Should one think of the transfer as a diffusion process or as an activated chemical reaction? Does the ion transfer from the water phase to the organic phase involve significant dragging of the hydration shell? If not, what is the mechanism by which the ion switches its solvation shell? What is the mechanism by which the hydration shell is built when the ion crosses from the organic phase to the aqueous phase?

Recent experimental and theoretical progress in the study of the liquid/liquid interface, which we described in section II, makes it possible to begin addressing the above questions. Most of the new insight gained about the process of ion transfer has been obtained by means of molecular dynamics computer simulation. Hayoun *et al*.[222] have studied the problem of a (neutral) Lennard-Jones atom transfer across a model liquid/liquid interface made of two identical Lennard-Jones liquids. They showed that the process can be understood as an activated crossing of a barrier, that is the result of the process of the switching of solvation shell members. Our focus here will be on ion transfer that is influenced by a free energy driving force, as is the case in electrochemical ion transfer experiments. Most of these experiments have been performed at the interface between water and 1,2-dichloroethane (DCE), and in the next section we will describe some recent work on this system. Following that, we will describe a relatively simpler microscopic model for ion transfer, which provides additional insight into the water/DCE system.

Because the water/DCE interface will play a major role in all of section V, we summarize the basic picture of its structure and dynamics which emerges from molecular dynamics computer simulation.[74] The neat water/DCE interface is sharp at the molecular level, but very rough. There is no region where water molecules are fully surrounded by DCE molecules or vise versa, but there are quite a number of water molecules with 1 or 2 hydrogen bonds with other water molecules. This picture can be summarized by noting that water "fingers" and DCE "fingers" protrude into the other phase. The process is a dynamic one. The water fingers can get as large as 8 Å, but finally they relax and other "fingers" are generated on the time scale of tens of picoseconds.

2. Ion Transfer at the Water/DCE Interface

Experimentally, ion transfer is monitored by setting up an equilibrium ion current under the influence of an external voltage. Depending on the polarity of the external field, the ion current can be from the aqueous phase to the organic phase or vice versa. Cyclic voltammetry diagrams (that can be analyzed using the same methodology as in the case of electrochemical processes at metal electrodes) show that the process is reversible. Microscopic simulation of this process is out of the question because of the need for a large enough system that will allow for

the establishment of a steady-state double-layer potential. Thus, the available microscopic treatments of this process are limited to the nonequilibrium transfer of a single ion under the influence of an external electric field. Before discussing the insight gained from these simulations, we consider the free energy profile for the ion transfer.

Despite the obvious importance of the free-energy profile for the ion along the distance normal to the liquid/liquid interface *A(z)*, very little is known about it. There is a large body of data[148] and some theory[216] about the *net free energy of transfer*, $A(z_{B1} - z_{B2})$, where z_{B1} and z_{B2} are positions in the bulk of the two phases, but not the full z dependence. Unlike the case of small ions at the liquid/vapor interface of water, where the main contribution to the free energy profile is electrostatic, here, in addition to the electrostatic contribution, there may be a significant difference in the amount of work to create the cavity in the water vs in the organic phase. Although this additional term is naturally included when the free energy profile is computed using molecular dynamics sampling, it is more instructive to examine the separate contributions[220] using approximate procedures. A discussion of the free-energy profile obtained from molecular dynamics sampling can be found in the original paper.[221]

In the top panel of Figure 11 we show two different model calculations for the electrostatic contribution to the free energy profile of Cl^- across the water/DCE interface, and an approximate calculation of the cavity term. One approximate calculation of the electrostatic contribution is based on the solution of the Poisson equation for a continuum dielectric model. The model consists of a water slab with a dielectric constant of 82.5 in contact with a DCE slab with a dielectric constant of 10, and a charged sphere representing the ion. The second approximate calculation is based on the molecular dynamics trajectories and a Gaussian model for the electrostatic potential fluctuations.[223] Later we will discuss a comparison between this model and a molecular dynamics calculation of the free energy profile in another system. Both electrostatic contributions are monotonically decreasing as one goes from the DCE to the water phase, reflecting the higher dielectric constant of the aqueous phase.

The approximate calculation of the cavity term is based on the scale particle theory[224−226] and its extension to the interface between two hard sphere liquids.[221,227] Briefly, this method is based on calculating the probability of finding a cavity of a given size at the interface. The top panel of Figure 11 shows that the cavity contribution is more positive in the aqueous phase, reflecting the hydrophobic nature of this cavity[228] and consistent with the higher solubility of rare gases in DCE than in water.[148]

The bottom panel of Figure 11 gives the total free-energy profile. The Gaussian model gives a net free energy of transfer of Cl^- from DCE to water of about −15 kcal/mol, compared with the continuum model, which gives −5 kcal/mol, and the experimental value of −12.4 kcal/mol.[148] The first free energy profile exhibits a significant barrier to the downhill transfer of about 3 kcal/mol. Although it is likely that this is

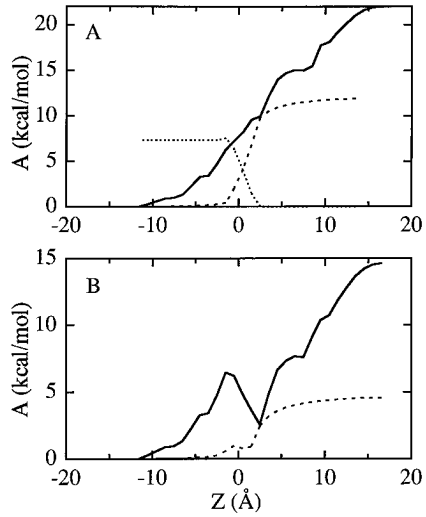

Figure 11. Free energy profile for an ion transfer across the water/1,2-dichloroethane interface. In panel A, the solid line is the electrostatic contribution calculated from the Gaussian fluctuation model and the molecular dynamics trajectories, the dashed line is the electrostatic contribution calculated using a continuum electrostatic model and the dotted line is the cavity contribution from a simple extension to the interfacial region of the scaled particle theory. In panel B, the sum of the electrostatic and the cavity terms are shown in solid line for the MD and in the dashed line for the continuum model. (Taken from ref 221. Copyright 1995 American Chemical Society.)

an approximate value, according to the model, its physical origin is simple: Due to the special structure of water, it is more difficult to create a cavity in this liquid,[228] and thus there is an initial free-energy cost as the ion begins to cross the interface. However, this is more than balanced when the ion is moved past the interface. It becomes fully solvated by the water, and so the net free energy of transfer is negative.

This simple picture is supported by the nonequilibrium molecular dynamics trajectories, a small sample of which are summarized in Figure 12. The left panels of this figure correspond to an average over 20 trajectories, in each of which the chloride ion starts in the center of the DCE phase and moves to the water phase under the influence of an external field of 0.2 V/Å. The right panels correspond to the reverse process, in which the ion starts in the bulk aqueous phase. Other values of the external electric field have been used, and for these the reader is referred to the original paper.[221] The left panels of Figure 12 show a rapid transfer of the chloride ion into the aqueous phase. The transfer is complete in a few tens of picoseconds because of a rapid build up of the hydration shell with an almost simultaneous breaking up the DCE solvation shell. The actual replacement of the solvation shell by water molecules is very rapid (a few picoseconds), and most of the time is spent with the ion looking for a water molecule that is weakly bound to the water phase. An examination of the animated trajectories shows that this is facilitated by water "fingers" whose head water molecule is "ready" to hydrate the ion. This separation of time scale is clear from the bottom left panel of Figure 12, where the first peak of the oxygen ion radial distribution function remains narrow at a fixed location. At lower electric field values this picture

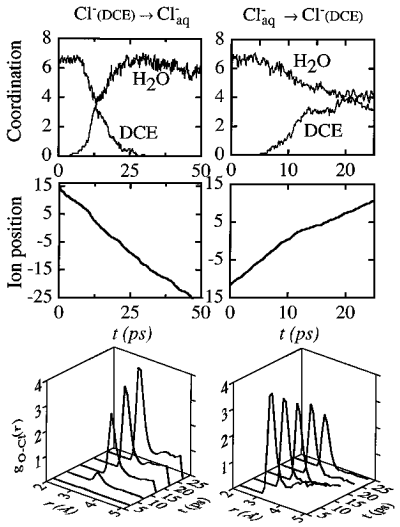

Figure 12. Nonequilibrium molecular dynamics trajectories of a chloride ion transfer across the water/1,2-dichloroethane interface at $T = 300$ K. The left three panels are for the transfer from the organic to the aqueous phase, and the three right panels are for the reverse process. The top panels gives the average (over 20 independent trajectories) time-dependent coordination number of the ion. The center panels show the average position of the ion. The bottom panels present the oxygen−ion radial distribution function. (Data taken from ref 221. Copyright 1995 American Chemical Society.)

is essentially the same, except that fewer ions are able to climb the barrier. These trajectories suggest that the source of the barrier is the entropic and energetic cost in finding a water "finger" which can "pull" in the ion. The actual switching of the first solvation shell members by water molecules is fast and not activated. In the next section, we will present a model which further supports this interpretation.

The right panels of Figure 12 describe the "uphill" transfer of the Cl^- ion from the water to the DCE phase. An external electric field of opposite polarity to the one used in the transfer from the DCE to water is necessary to overcome the significant free energy difference. Although the magnitude of the external field is the same as before, the process is much slower. This external field is not strong enough to overcome the barrier on the simulation time scale, and most of the ions are still in the interface region. It is interesting to note that although on average, by the end of the run, the ion is 10 Å into the DCE phase, the solvation shell still contains a significant number of water molecules (top right panel). The radial distribution function shows the disappearance of the second hydration shell, but the first peak is still significant. An examination of individual trajectories shows that the ion is solvated by water molecules, but that the solvation complex is in the DCE phase and connected to the water phase by a "chain" of water molecules. This causes the interface to be significantly perturbed.

The transfer from the water to the organic phase clearly involves dragging the ion hydration shell into the organic phase. This is just another example of the tendency to keep the hydration shell intact, as we have previously discussed. The development of a "chain" of water molecules connecting the hydrated ion (in the DCE phase) to the bulk water can also be thought of as the time reversal of the process by which the ion is transferred from the DCE phase to the water with the help of water "fingers". These fingers are the most dramatic manifestation of the role played by surface roughness in facilitating ion transfer.

3. A Simple Model of Ion Transfer

The study of ion transfer across the water/DCE interface described in the last section illustrates the important role played by the water structure in creating a barrier for the transfer and in facilitating the transfer with the help of surface roughness. We describe here another microscopic model which also involves a significant free energy driving force, but which lacks the unique features of the water surface. We will see that in this system, the ion transfer is fast and activationless.

The system includes 256 polar diatomic molecules (with a dipole moment of 3 Debye) in contact with 256 nonpolar diatomic molecules. All the atoms in the system have the same Lennard-Jones parameters. The two liquids are immiscible because of the favorable interactions among the polar molecules. The ion is also described by the same Lennard-Jones parameters, and its charge is +1. More details about the system can be found in the original paper.[219]

The free energy profile for the ion in this system was calculated by an umbrella sampling procedure similar to the method discussed earlier for the ion at the water liquid/vapor interface. It is shown in Figure 13. The nonpolar liquid occupies approximately the region $Z > 0$, and the polar liquid is in the $Z < 0$ region. The molecular dynamics result shows a significant driving force without any barrier. The dotted line shows the solution to the Poisson equation for a sharp dielectric model with a dielectric constant of 1 for the nonpolar liquid and 35 for the polar liquid. The results of the approximate Gaussian model are almost identical to the molecular dynamics results.[219] Note also that if we apply the simple model for estimating the cavity contribution, there would be no difference between the cavity work in the two liquids. Thus, the simple approximate

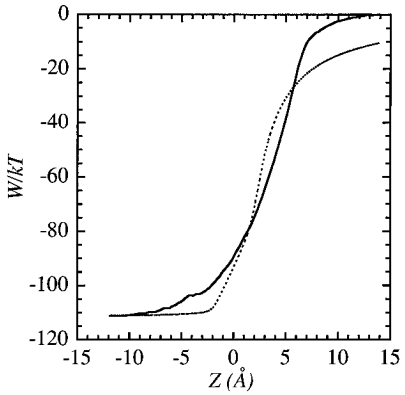

Figure 13. The free energy profile for an ion transfer across a simple polar liquid/nonpolar liquid interface: solid line, molecular dynamics calculations using umbrella sampling; dotted line, continuum electrostatic model. (Data taken from ref 219. Copyright 1992 American Institute of Physics.)

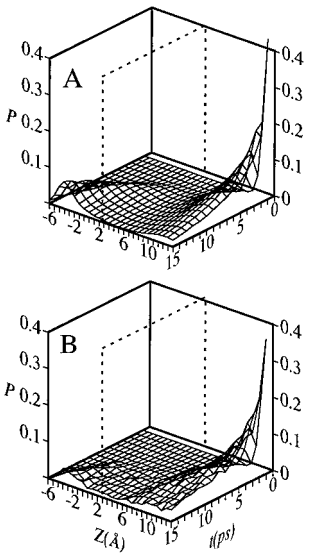

Figure 14. Time-dependent probability distribution for ion transfer across the simple liquid/liquid interface. Z is the distance along the interface normal, and $Z > 0$ corresponds to the region occupied by the nonpolar liquid. Panel A shows the solution of a diffusion equation on the potential of mean force of Figure 13. Panel B shows the results of 500 independent molecular dynamics trajectories for an ion that starts at the center of the nonpolar liquid. (Taken from ref 219. Copyright 1992 American Institute of Physics.)

model for calculating the profile discussed in the last section would also give a monotonically decreasing free energy profile.

This picture of an activationless transfer across the interface, suggested by the equilibrium free-energy calculation and the simple model, is also supported by extensive nonequilibrium trajectory calculations. Because of the simplicity of the system and the fact that the transfer is fast, a large number (500) of trajectories can be used to get an accurate description of the ion dynamics. In Figure 14, the time-dependent probability distribution for the ion position $P(z,t)$ from the molecular dynamics trajectories (panel B) is compared with a numerical solution of a one-dimensional diffusion equation:[229]

$$\frac{\partial P(z,t)}{\partial t} = \frac{\partial^2[D(z)P(z,t)]}{\partial^2 z} + \beta\frac{\partial}{\partial z}D(z)W'(z)P(z,t) \quad (9)$$

in which $W'(z)$ is the spatial derivative of the free energy profile, $D(z)$ is the distance-dependent diffusion constant (obtained from the later motion of the ion in the molecular dynamics trajectories), and $\beta = 1/kT$. The quantitative agreement between the two calculations further supports the activationless, simple diffusive nature of the ion transfer in this system. The transfer of the ion in most of the 500-member ensemble of trajectories is complete in about 10 ps, as can be seen from the near exponential decay of the initial sharp peak and the simultaneous buildup of the broader peak in the bulk polar solvent.

This model shows that ion transfer between simple non-hydrogen bonding liquids can be understood as a diffusion of a particle under the influence of an external force field, in contrast with a transfer across the water/DCE interface. The theoretical understanding of ion transfer in realistic systems in which larger ions cross the interface with a small free energy of transfer, is a challenge for future work.

C. Electron Transfer

Electron transfer (ET) reactions at the interface between two immiscible electrolyte solutions and at the metal/electrolyte solution interface are some of the most important interfacial chemical reactions. However, they are relatively poorly understood for some of the same reasons that ion transfer is not well understood—a lack of knowledge about the microscopic structure of the interface and the difficulty of carrying out experiments sensitive enough to these microscopic features. In contrast to ion transfer, though, the basic theory of electron transfer is well developed,[203,230−232] and so we limit the discussion here to new microscopic developments about ET reactions at liquid interfaces.

1. Electron Transfer at the Liquid/Liquid Interface

In recent years, information about ET reactions at the liquid/liquid interface is beginning to be available for the first time.[27,233−236] Theoretical work in this area is also very limited and very recent, because very little kinetic data are available yet. This work includes a few continuum model calculations of the reorganization free energy λ for an outer-sphere ET reaction,[237−239] and a few molecular dynamics calculations[240,241] of λ and of solvent dynamics following photochemically induced interfacial ET.[242] We review these developments in this section.

Marcus presented a continuum model calculation of the reorganization free energy at the interface between two immiscible liquids[239] and used it to estimate the rate in the nonadiabatic limit.[243,244] The calculation of the reorganization free energy[239] is along the same lines as Marcus' original calculation of the free energy of nonequilibrium polarization,[245] and below we only summarize the assumptions and give the results.

Consider an electron donor (D) and an electron acceptor (A) that are adsorbed at the interface between two immiscible liquids. D and A are structureless, so that the electron transfer between them, $DA \rightarrow D^+A^-$, involves only outer-sphere solvent reorganization. The contribution of inner vibrational modes can be added in the usual way[245] by including the change in the equilibrium bond length and force constant between the reactants and products. However, since these are expected to be only mildly affected by the interface, we do not include this contribution here. The interface is assumed to be mathematically sharp, with the A and the D each restricted to being in a separate phase. Local electrostatics is also assumed. The reorganization free energy is found to be

$$\lambda = {}^1/_2(\Delta q)^2\left[\frac{a_1^{-1} - \gamma_\infty/2d_1}{\epsilon_1^\infty} - \frac{a_1^{-1} - \gamma_0/2d_1}{\epsilon_1^0} + \right.$$

$$\left.\frac{a_2^{-1} - \gamma_\infty/2d_2}{\epsilon_2^\infty} - \frac{a_2^{-1} - \gamma_0/2d_2}{\epsilon_2^0} - \frac{4R^{-1}}{\epsilon_1^\infty + \epsilon_2^\infty} + \frac{4R^{-1}}{\epsilon_1^0 + \epsilon_2^0}\right] \quad (10)$$

Reactant i ($i = 1, 2$) with radius a_i is located in phase i at a distance d_i from the interface, and R is the distance between them. Δq is the magnitude of the charge transfer, and $\gamma_\nu = (\epsilon_2^\nu - \epsilon_1^\nu)/(\epsilon_2^\nu - \epsilon_1^\nu)$, $\nu = 0, \infty$, where ϵ_i^∞ and ϵ_i^0 are the infinite frequency and static dielectric constants of phase i, respectively. This expression reduces to the normal bulk liquid expression[246] when one substitutes $\epsilon_1^0 = \epsilon_2^0$ and $\epsilon_1^\infty = \epsilon_2^\infty$.

The rate constant for the electron-transfer reaction was estimated by Marcus in the nonadiabatic limit within the linear response approximation, and it is given by

$$k_r = \kappa \nu V_r e^{-\beta \Delta G^\ddagger} \tag{11}$$

where κ is the Landau−Zener factor for the nonadiabatic transitions[247] between the two diabatic electronic states, and ν is the molecular frequency, which is determined from the equilibrium solvent fluctuations in the reactant state. V_r accounts for all of the possible configurations of the reactant pair per unit area of the interface, taking into account their spherical size and the fact that they cannot cross the interface:

$$V_r = 2\pi(a_1 + a_2)(\delta R)^3 \tag{12}$$

where δR is a length scale which arises from the weighting of the reactants' configuration by the exponential form of the electronic coupling between them, $e^{-R/\delta R}$. (This assumes that the nonadiabatic regime applies to all values of R, which must be incorrect for small R.) The activation energy $\Delta G^\ddagger$ is given by[239,243,244]

$$\Delta G^\ddagger = W_r + \frac{(\lambda + \Delta G^0 + W_p - W_r)^2}{4\lambda} \tag{13}$$

where G^0 is the standard reaction free energy, W_r is the reversible work required to bring the reactants from the bulk of each phase to the interface, and $-W_p$ is the reversible work required to separate the products.

To apply this formula, one requires quite a number of unknown parameters. Marcus showed that the reorganization free energy may be estimated from the rate constant of the half reaction at the solution/metal interface.[243] This and other assumptions give reasonable agreement with the experimental rate constant for the reaction between the $Fe(CN)_6^{4-/3-}$ couple in water and the $Lu(PC)_2^{+/2+}$ (hexacyanoferrate-lutetium biphthalocyanine) couple in DCE. Unfortunately, reasonable agreement can also be achieved if one assumes that the interface region is a broad homogeneous phase. Other tests of the theory must await more experimental data.

One of the main contributions of the microscopic treatment of the interfacial ET is that it can help us check the basic assumptions of the above simple theory. The main assumptions of the continuum model that can be easily checked are the linear response approximation, the structure of the interface, and the geometrical distribution of the reactants at the interface, as previously discussed. The linear response assumption is at the heart of the calculation of the reorganization free energy, and we will focus on it first.

Since our main goal here is to focus on the interfacial effects, we choose to consider a simple two-state approach for the microscopic treatment of ET.[248−253] According to this approach, the electron-transfer reaction can be viewed as a transition between two localized electronic states—the reactant state and the product state, $|R\rangle$ and $|P\rangle$, respectively. The energies of these two states, E_R and E_p, fluctuate because of solvent motion. In the Born−Oppenheimer and Frank−Condon approximation, the electron transfer occurs when the energy of the two states is the same. The probability of observing a solvent fluctuation that equalizes the energy of the two states can be represented by using the concept of "solvent coordinate". This coordinate, which we will use as the reaction coordinate, is defined as

$$X(\mathbf{r}) = E_P - E_R \tag{14}$$

where $\mathbf{r}$ is the positions of all solvent atoms. For example, if the reactants and products are spherical, structureless atoms, which interact with the liquid atoms through the same Lennard-Jones potentials, and the charge transfer is of one electron, then X is just the difference in the electrostatic potential induced by the liquid at the location of the reactants. The probability $P(x)$ that $X(r)$ is equal to some value x (where x = 0 is the transition state) is

$$P_\nu(x) = \langle \delta[X(\mathbf{r}) - x] \rangle_\nu \tag{15}$$

where the ensemble average is over the reactant ($\nu = R$) or the product ($\nu = P$) state. The free energies

$$G_\nu(x) = -\beta^{-1} \ln P_\nu(x) \tag{16}$$

represent the reversible work needed to change the solvent polarization in order to have a specific value x of $X(\mathbf{r})$. Equation 13 for the activation free energy is based on the assumption that the solvent free energies $G_R(x)$ and $G_P(x)$ are parabolai with identical curvatures. This assumption can be directly checked by calculating the free energies using molecular dynamics umbrella sampling, with the help of a biasing potential which allows for evaluation of the free energy far away from the equilibrium state.[240,241,251,253] This has been done for ET reactions in bulk water[251,253] and at the interface between two simple liquids[240] (this interface was discussed in the section on ion transfer).

Figure 15 shows the solvent free energies for an ET reaction between two Lennard-Jones spheres (σ = 5 Å, ϵ = 0.1 kcal/mol) located at the water/DCE interface, compared with the free energies in bulk water.[241] The results in the bulk are similar to what King and Warshel obtained.[253] The free energy calculated from the molecular dynamics umbrella sampling begins to deviate from the value predicted by linear response only far from the minimum of each state. The deviation reflects both the nonlinear character of the solvent and the different curvatures of the parabolai. The curvature for the ion pair is smaller than that for the neutral pair due to the

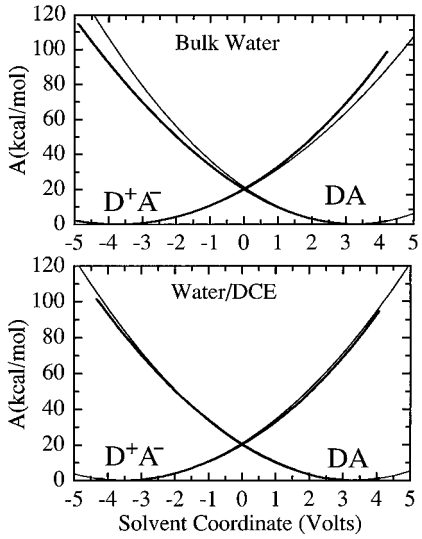

Figure 15. The solvent free energy function for the electron transfer reaction $D^+ + A^- \rightarrow DA$ in bulk water (top panel) and at the water/1,2-dichloroethane interface: thick lines, umbrella sampling calculations; thin lines, parabolic fit. (Taken from ref 227. Copyright 1994 American Chemical Society.)

water structure breaking the effect of the ions, which increases the fluctuations of the solvation shell. Despite the deviations, the activation free energy predicted by the molecular dynamics results is almost identical to the one predicted by the quadratic approximation for the case of zero reaction free energy, a region where most ET rate measurements are carried out.

The agreement between the full molecular dynamics calculations and the linear response for ET at the water/DCE interface is even better. It is, in fact, almost perfect. Apparently, the structure-breaking effect of the ions is much weaker at the interface, probably due to the stronger hydrogen bonding there. However, no systematic study of these issues has been carried out.

It is possible to compare the reorganization free energy calculated from the continuum dielectric model (eq 10) with the value of 80 kcal/mol obtained from the molecular dynamics data of Figure 15. Using 1 for the infinite frequency dielectric constant and 82.5 and 10 for the static ones (for water and DCE, respectively), the value of the Lennard-Jones σ as the diameter of each solute, the value of $R = 6$ Å and the average distance of each solute from the Gibbs surface obtained from the molecular dynamics (which corresponds to an average angle of 45° between the vector connecting the ion pair and the interface normal), one gets $\lambda = 74$ kcal/mol, which is in surprisingly good agreement with the molecular dynamics results. The agreement is surprising because one can also check in a detailed way the assumptions under which eq 10 was derived and find that these assumptions are not really justified. For example, the interface is very rough, and the reactants can approach at a wider angle than the maximum value of $\cos^{-1}[(a_1 + a_2)/R]$ predicted by the sharp model. More interesting is that the electrostatic potentials induced by each liquid at the location of the ions, and calculated from the molecular dynamics trajectories and from the continuum model, are in poor agreement with each other. One finds that the water potentials are underestimated by the continuum model (due to the neglect of the specific hydration structure and the near perfect alignment of the water dipole around the ion), but that the DCE potential is overestimated, so that the total potential is in reasonable agreement with the continuum model.[172,227]

We conclude this section with a brief discussion of solvent dynamic response. In the context of solvation dynamics, we have already discussed how the solvent response to a sudden change in the solute charge distribution can be used as a test of continuum dielectric models of the interface. More generally, this response can be used as a probe of the interface structure and dynamics. Solvent dynamical response has been the focus of many experimental studies in recent years because of the role that this response can play in the rate of very fast reactions.[153,154,203,254] As new experimental techniques are beginning to be applied to ET at the liquid/liquid interface, the issue of solvent dynamics will be relevant on this front as well. Since there are no fast time-resolved studies of ET at the liquid/liquid interface, we only mention a few molecular dynamics studies of this subject, focusing again on interfacial effects.

A detailed study of the solvent response to the charge separation reaction $A + D \rightarrow A^- + D^+$ and to the reverse, charge recombination reaction, taking place at the interface between two immiscible liquids has been carried out by Benjamin.[242] The interface, which was discussed earlier, is between a model diatomic nonpolar solvent and a diatomic polar solvent. Ion pairs and neutral pairs with different fixed orientations relative to the interface have been studied. It was found that the relaxation at the interface for the charge separation reaction is much slower than in the bulk, in contrast to a prediction of the continuum electrostatic model. The main reason for this is that when an ion pair is suddenly created at the interface, large structural rearrangements of surface dipoles are needed to solvate it. In this liquid/liquid system, the dipoles' motion is restricted at the interface but less so in the bulk.

An example of a similar reaction at the water/DCE interface[241] is shown in Figure 16. The total solvent response (defined in eq 7), as well as the individual contribution of water and of DCE, are shown for the charge separation and charge recombination reactions. The total correlation function includes a very rapid component, which accounts for about 60% of the full decay in the charge recombination reaction, but only about 30% of the full decay following the charge separation reaction. An examination of the individual contribution of the two liquids shows that the initial rapid component is mainly due to the water librational motion. A comparison of the water contribution to the total contribution shows that even at a later time most of the relaxation is due to water reorientation. This is not surprising, as even at the interface the ions are mostly solvated by the water. It is expected that as the charge centers are buried deeper in the organic phase, the total response will more resemble the response that is characteristic of DCE. Thus, monitoring the solvent response may

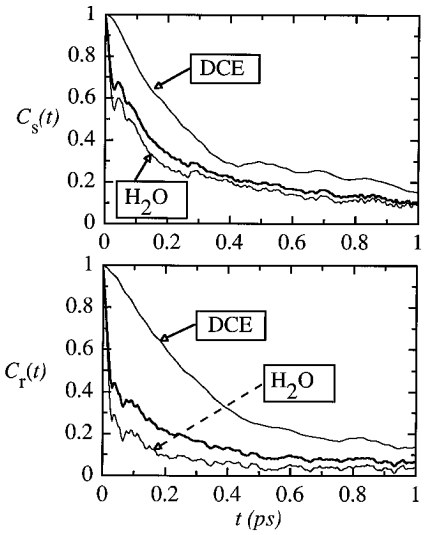

Figure 16. The solvent relaxation following a photochemically induced electron transfer at the water/1,2-dichloroethane interface. The top panel corresponds to the charge separation reaction $DA \rightarrow D^+ + A^-$ and the bottom panel to the reverse, charge recombination reaction. In each panel, the individual contribution of the two liquids and the total response are shown. (Taken from ref 227. Copyright 1994 American Chemical Society.)

give information about the degree by which the charges are solvated by each liquid, the location of the charges, and the structure of the interface. For example, a very sharp interface will show a marked sensitivity of the solvent response to the location of the charge centers, whereas a broad interfacial region will result in a solvent response that is nearly independent of the location of the probe.

2. Electron Transfer at the Metal/Water Interface

ET reactions at the solution/metal interface have been the focus of numerous experimental and theoretical studies, and many aspects of the problems have been reviewed recently.[45,52] In keeping with the microscopic emphasis of this review, we only focus on recent developments which explicitly take into account the microscopic structure of the solvent.

The theoretical study of ET at the solution/metal interface is complicated because the electronic structure of the metal plays a major role in this reaction. This was recognized very early, and significant effort has been made to take into account the interaction of the metal electrons with the solute and with the pure solvent. However, until recently the solvent has been described using a continuum dielectric model or a collection of harmonic oscillators. Given the significant progress made in recent years in the microscopic molecular description of liquids at solid surfaces, it is of interest to combine a realistic quantum mechanical treatment of the ET reaction with a realistic microscopic description of the solvent.

The simplest possible approach includes the full microscopic description of the solvent but treats the ET as an effective two-state problem. This approach is mainly useful in elucidating the effect of the interface on the solvent reorganization free energy. Most of the progress made to date on ET at the metal/water interface with a microscopic description of the solvent has been using this two-state model, although there are some very recent developments which go beyond this. These topics will be reviewed in this section.

Within the two-state model, the theoretical description of ET at the water/metal interface is similar to the one discussed in the last section. Instead of an ion pair we have a single ion (or a neutral solute) adsorbed at the metal surface. One diabatic state has the electron localized on the ion, while the electrons in the metal occupy the orbitals up to the Fermi level. In the other state, the electron is added to one of the empty metal orbitals (whose location may be influenced by solvent dipoles, the solvent electronic wave function and the external potential drop across the electrode), and the ion orbital is empty. Thus, the metal is considered a second "big ion". This model ignores electronic transitions in the metal, which have been included in more detailed descriptions of ET using simplified solvent models.[255−261] The main utility of this two-state model is in examining the solvent contribution to the reorganization free energy, which is a main ingredient in the activation free energy for the ET reaction.

The first attempt to study ET at the interface between a realistic microscopic model of water and a "classical" metal surface was by Halley and Hautman[262] and by Curtiss *et al.*[263] In this work, the metal surface was treated as a simple flat Lennard-Jones solid, and the fluctuations in the water were used to calculate the rate of nonadiabatic electron transfer. The free energy curves for the electron transfer were estimated by linear response theory. This calculation was limited to a low activation free energy, and the transitions were treated in the Born approximation.

Straus and Voth[264] used an umbrella sampling procedure to compute the full-solvent free-energy profile for the ET reaction $Na^+ + e^- \rightarrow Na$ at the water/Pt interface, using the potential of Raghaven and Berkowitz.[88] This allowed them to check the validity of the linear response theory. They found that the solvent free energies in the presence of the ion are well approximated by a parabola, but that a noticeable discrepancy exists in the case of the neutral atom. In addition, they found that the reorganization free energy, determined from a hypothetical calculation of the solvent free energy in bulk water, is almost identical to the value at the interface, a result that may be useful for estimation of this reorganization free energy from statistical mechanical theories in bulk liquids.

Rose and Benjamin[265,266] calculated the solvent free-energy curve for the reactions $Fe^{3+} + e^- \rightarrow Fe^{2+}$ and $Fe^+ + e^- \rightarrow Fe$ at the charged and uncharged water/Pt(100) interface using umbrella sampling. In general, they found that the linear response approximation is reasonable for all cases. The largest deviation was found for the solvent free energy in the presence of the neutral atom. As an example, we show in Figure 17 the results for the solvent free energies for the Fe^{2+} and Fe^{3+} ions at the surface and in the bulk. The application of a strong electric field does not make any appreciable change in the shape of the free energy curves.[266]

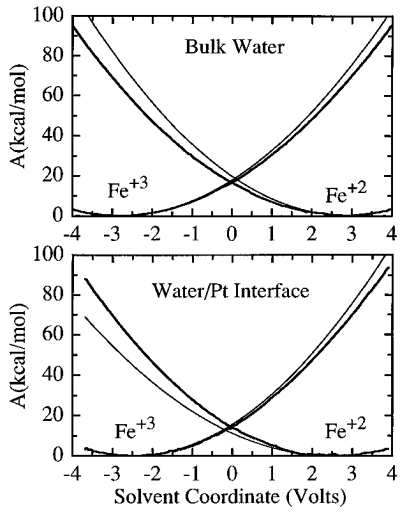

Figure 17. The solvent free energy functions for the electron transfer reaction $Fe^{3+} + e^- \rightarrow Fe^{2+}$ in bulk water (top panel) and at the water/Pt interface: thick lines, umbrella sampling calculations; thin lines, parabolic fit.

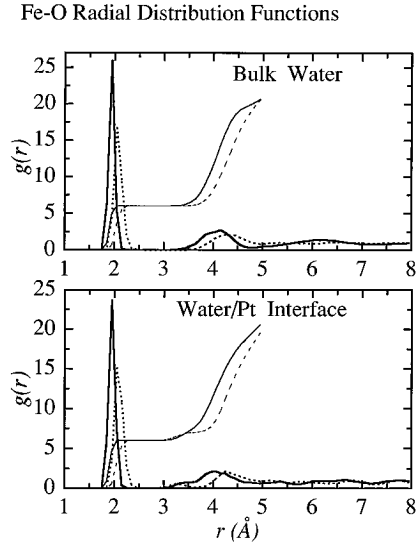

Figure 18. Oxygen ion radial distribution functions and running coordination numbers for Fe^{2+} (dotted and dashed lines, respectively) and for Fe^{3+} (solid thick and thin lines, respectively) in bulk water and at the water/Pt interface.

Some insight into the fact that there is only a minor surface effect on the shape of the free energy curves, despite the significant difference in the structure and the dynamics of the interfacial water, can be obtained from an examination of the structure of the ions' hydration shell. For both Fe^{2+} and Fe^{3+} ions in the bulk and at the interface, there is an almost perfect octahedral structure of water molecules.[265] The small differences in the water structure are demonstrated in Figure 18, in which the oxygen ion radial distribution functions for both ions in the bulk and at the interface are shown. As expected, the radial distributions for the higher charge ion are more peaked. The difference between the bulk and the interface is very small. The only noticeable difference between them is in the location of the minimum of the free energy of the neutral atom (Fe), which simply reflects the smaller solvation energy at the surface.[266] This change in the location of the minimum results in a change in the activation free energy because of a corresponding change in the crossing point of the two parabolas. Similar results have been observed by Xia and Berkowitz,[267] who found that the shift in the location of the minimum of the solvent free energy for I^- is especially large due to a partial lose in the hydration shell.

Rose and Benjamin[265] used the diabatic free energy curve to calculate the rate constant in the diabatic limit as a function of the electrode/solution potential difference. This was done using a surface-hopping procedure, which involves the solution of the time-dependent Schrodinger equation in the Born approximation in the vicinity of the crossing point.[262,268] Rose and Benjamin also developed a Hamiltonian for the adiabatic electron-transfer reaction, which is believed to be the regime for most electron-transfer reactions at the electrode/electrolyte interface.[256] This Hamiltonian is obtained by diagonalization of the two-state model Hamiltonian. The resulting potential energy surface has been used to compute the double-well free-energy governing the adiabatic ET reaction as a function of electronic coupling and the electrode/solution potential difference. The dynamics of barrier recrossings were calculated using the standard reactive flux correlation function (discussed earlier). They were found to be significant (transmission coefficient as low as 0.4), but were found to be very similar to the dynamics in bulk water. The above examples suggest that surface effects due to the unique interfacial solvent structure are minimal for ET reactions that involve small and/or highly charged ions.

An attempt to go beyond the two-state model was presented recently by Straus, Calhoun, and Voth.[269] They used an Anderson−Newns-like Hamiltonian to develop an adiabatic model for the reaction $Fe^{3+} + e^- \rightarrow Fe^{2+}$ at the water/Pt(111) surface. The adiabatic classical free-energy curve for the reaction was computed using umbrella sampling, and reactive flux calculations were performed to determine the effect of transition state recrossings on the classical adiabatic rate constant. As in the case studied by Rose and Benjamin, the recrossings were significant. An important contribution of the work by Straus, Calhoun and Voth was to calculate the quantum adiabatic free energy curves by quantizing the water model using Feynman path integral techniques. They found that the activation free energy and the reaction free energy for the electron-transfer process can be significantly affected by the water quantization.

We finally note that a first attempt to combine both the electronic structure of the metal surface and the molecular structure of the solvent has recently been presented by Price and Halley.[270] To date, they have used it only to calculate the structure of the neat solvent at the interface, but the inclusion of ions and perhaps even ET reactions seems feasible.

VI. Conclusions and Outlook

The liquid interface region has been shown to have unique properties. Some of these can be described with the use of bulk liquid concepts, such as effective density and dielectric constant. Some properties do not have a bulk counterpart, such as surface roughness and microscopic structural constraints (like

molecular orientation). Each one of these properties can significantly influence and modify the solvation of molecules and the equilibria and rate of chemical reactions.

The experimental and theoretical studies of chemical reactions at liquid interfaces at the microscopic level are still in their infancy. There is a need for new experimental data in order to provide a more detailed and direct probe of reaction dynamics. In particular, time-resolved studies at liquid interfaces, which have been recently reported, need to be expanded to include systematic studies of different reactions and different solvents.

On the theoretical side, progress is needed in three areas. First, a simulation of more realistic systems with more realistic potentials are would be useful. For example, we need to know how polarizability affects the structure of the neat water/organic phase interface, and how this influences ion transfer and solvation. Second, an improvement in the simple continuum models to account for the microscopic structure of the interface would be very useful. For example, can one account for the solvation free energy of ions at interfaces, and at the same time correctly describe the solvent dynamic response by considering a hydration complex within a dielectric continuum model for the interface? Third, despite the promising progress in statistical mechanical theories of inhomogeneous liquids, this progress has not been put to use in studying the behavior of solute at the interface. For example, can one combine a microscopic bulk description of the solvation complex with a mean field theory of the liquid/vapor interface in order to compute reliable ion adsorption free energies?

Progress in the above area will likely bring our level of understanding of liquid interfacial chemical reactions to what we have grown accustomed to for chemical reactions in bulk liquids.

VII. Acknowledgments

This work was supported by the National Science Foundation (Grant CHE-9221580), by the Petroleum Research Fund administered by the American Chemical Society (Grant 27255-AC), and by the Senate of the University of California at Santa Cruz. I would like to thank my collaborators: Daniel Rose, Karl Schweighofer, David Michael, Michael Wilson, and Andrew Pohorille. I am also grateful to Rob Corn, Gil Nathanson, and Liem Dang for helpful discussions.

VIII. References

(1) Bockris, J. O'M.; Gonzalez-Martin, A. In *Spectroscopic and Diffraction Techniques in Interfacial Electrochemistry*; Gutierrez, C., Melendres, C., Eds.; Kluwer Academic Publishers: Dordrecht, 1990.
(2) Bard, A. J.; Faulkner, L. R. *Electrochemical methods: fundamentals and applications*; Wiley: New York, 1980.
(3) Starks, C. M.; Liotta, C. L.; Halpern, M. *Phase Transfer Catalysis*; Chapman & Hall: New York, 1994.
(4) Arai, K.; Ohsawa, M.; Kusu, F.; Takamura, K. *Bioelectrochem. Bioenerg.* **1993**, *31*, 65.
(5) Gennis, R. B. *Biomembranes*; Springer: New York, 1989.
(6) *The Chemistry of Acid Rain: Sources and Atmospheric Processes*; Johnson, R. W., Gordon, G. E., Ed.; American Chemical Society Symposium Series; American Chemical Society: Washington, DC, 1987.
(7) Adamson, A. W. *Physical Chemistry of Surfaces* 5th ed.; Wiley: New York, 1990.
(8) Shen, Y. R. *The Principles of Nonlinear Optics*; Wiley: New York, 1984.
(9) Eisenthal, K. B. *Annu. Rev. Phys. Chem.* **1992**, *43*, 627.
(10) Grubb, S. G.; Kim, M. W.; Raising, T.; Shen, Y. R. *Langmuir* **1988**, *4*, 452.
(11) Corn, R. M.; Higgins, D. A. *Chem. Rev.* **1994**, *94*, 107.
(12) Ong, S.; Zhao, X.; Eisenthal, K. B. *Chem. Phys. Lett.* **1992**, *191*, 327.
(13) Fischer, P. R.; Daschbach, J. L.; Richmond, G. L. *Chem. Phys. Lett.* **1994**, *218*, 200.
(14) Bhattacharyya, K.; Castro, A.; Sitzmann, E. V.; Eisenthal, K. B. *J. Chem. Phys.* **1988**, *89*, 3376.
(15) Sitzmann, E. V.; Eisenthal, K. B. *J. Phys. Chem.* **1988**, *92*, 4579.
(16) Bhattacharyya, K.; Sitzmann, E. V.; Eisenthal, K. B. *J. Chem. Phys.* **1987**, *87*, 1442.
(17) Zhao, X. L.; Subrahmanyan, S.; Eisenthal, K. B. *Chem. Phys. Lett.* **1990**, *171*, 558.
(18) Meech, S. R.; Yoshihara, K. *Chem. Phys. Lett.* **1990**, *174*, 423.
(19) Morgenthaler, M. J. E.; Meech, S. R. *Chem. Phys. Lett.* **1993**, *202*, 57.
(20) Castro, A.; Ong, S.; Eisenthal, K. B. *Chem. Phys. Lett.* **1989**, *163*, 412.
(21) Castro, A.; Bhattacharyya, K.; Eisenthal, K. B. *J. Chem. Phys.* **1991**, *95*, 1310.
(22) Vogel, V.; Mullin, C. S.; Shen, Y. R.; Kim, M. W. *J. Chem. Phys.* **1991**, *95*, 4620.
(23) Higgins, D. A.; Corn, R. M. *J. Phys. Chem.* **1993**, *97*, 489.
(24) Higgins, D. A.; Naujok, R. R.; Corn, R. M. *Chem. Phys. Lett.* **1993**, *213*, 485.
(25) Naujok, R. R.; Higgins, D. A.; Hanken, D. G.; Corn, R. M. *J. Chem. Soc., Faraday Trans.* **1995**, *91*, in press.
(26) Sitzmann, E. V.; Eisenthal, K. B. *J. Chem. Phys.* **1989**, *90*, 2831.
(27) Kott, K. L.; Higgins, D. A.; McMahon, R. J.; Corn, R. M. *J. Am. Chem. Soc.* **1993**, *115*, 5342.
(28) Superfine, R.; Huang, J. Y.; Shen, Y. R. *Phys. Rev. Lett.* **1991**, *66*, 1066.
(29) Du, Q.; Superfine, R.; Freysz, E.; Shen, Y. R. *Phys. Rev. Lett.* **1993**, *70*, 2313.
(30) Du, Q.; Freysz, E.; Shen, Y. R. *Science* **1994**, *264*, 826.
(31) Heinz, T. F.; Tom, H. W. K.; Shen, Y. R. *Phys. Rev. A.* **1983**, *28*, 1883.
(32) Goh, M. C.; Hicks, J. M.; Kemnitz, K.; Pinto, G. R.; Bhattacharyya, K.; Eisenthal, K. B.; Heinz, T. F. *J. Phys. Chem.* **1988**, *92*, 5074.
(33) Conboy, J. C.; Daschbach, J. L.; Richmond, G. L. *J. Phys. Chem.* **1994**, *98*, 9688.
(34) Conboy, J. C.; Daschbach, J. L.; Richmond, G. L. *Appl. Phys. A* **1994**, *59*, 623.
(35) Messmer, M. C.; Conboy, J. C.; Richmond, G. L. *J. Am. Chem. Soc.* **1995**, *117*, 8039.
(36) Beaglehole, D. In *Fluid Interfacial Phenomena*; Croxton, C. A., Ed.; Wiley: New York, 1986.
(37) Pershan, P. S. *Faraday Discuss. Chem. Soc.* **1990**, *89*, 231.
(38) Schwartz, D. K.; Schlossman, M. L.; Kawamoto, E. H.; Kellogg, J. G.; Pershan, P. S.; Ocko, B. M. *Phys. Rev. A* **1990**, *41*, 5687.
(39) Lee, L. T.; Langevin, D.; Farnoux, B. *Phys. Rev. Lett.* **1991**, *67*, 2678.
(40) Wirth, M. J.; Burbage, J. D. *J. Phys. Chem.* **1992**, *96*, 9022.
(41) Kovaleski, J. M.; Wirth, M. J. *J. Phys. Chem.* **1995**, *99*, 4091.
(42) Mirkin, M. V.; Fan, F.-R. F.; Bard, A. J. *Science* **1992**, *257*, 364.
(43) Sperline, R. P.; Freiser, H. *Langmuir* **1990**, *6*, 344.
(44) *Fluid Interfacial Phenomena*; Croxton, C. A., Ed.; Wiley: New York, 1986.
(45) *Spectroscopic and Diffraction Techniques in Interfacial Electrochemistry*; Gutierrez, C., Melendres, C., Eds; NATO ASI Series vol. 320. Kluwer Academic Publishers: Dordrecht, 1990.
(46) Fleming, G. R. *Chemical Applications of Ultrafast Spectroscopy*; Oxford University: New York, 1986.
(47) Hynes, J. T. In *The Theory of Chemical Reactions*; Baer, M., Ed.; CRC Press: Boca Raton, FL, 1985; Vol. 4.
(48) Whitnell, R. M.; Wilson, K. R. In *Reviews in Computational Chemistry*; Lipkowitz, K. B., Boyd, D. B., Eds.; VCH: New York, 1993.
(49) Croxton, C. A. *Statistical Mechanics of the Liquid Surface*; Wiley: New York, 1980.
(50) Rowlinson, J. S.; Widom, B. *Molecular Theory of Capillarity*; Clarendon: Oxford, 1982.
(51) Percus, J. K.; Williams, G. O. In *Fluid Interfacial Phenomena*; Croxton, C. A., Ed.; Wiley: New York, 1986.
(52) In *Fundamentals of Inhomogeneous Fluids*; Henderson, D., Ed.; Marcel Dekker: New York, 1992.
(53) Pohorille, A.; Wilson, M. A. *J. Mol. Struct. (Theochem)* **1993**, *284*, 271.
(54) Zhu, S.-B.; Singh, S.; Robinson, G. W. *Adv. Chem. Phys.* **1994**, *85*, 627.
(55) Conway, B. E. In *The Liquid State and its Electrical Properties*; Kunhardt, E. E., Christophorou, L. G., Luessen, L. H., Eds.; Nato ASI series B; Plenum: New York, 1988; Vol. 193.

(56) Townsend, R. M.; Gryko, J.; Rice, S. A. *J. Chem. Phys.* **1985**, *82*, 4391.
(57) Allen, M. P.; Tildesley, D. J. *Computer Simulation of Liquids*; Clarendon: Oxford, 1987.
(58) Wilson, M. A.; Pohorille, A.; Pratt, L. R. *J. Phys. Chem.* **1987**, *91*, 4873.
(59) Wilson, M. A.; Pohorille, A.; Pratt, L. R. *J. Chem. Phys.* **1988**, *88*, 3281.
(60) Nijmeijer, M. J. P.; Bakker, A. F.; Bruin, C.; Sikkenk, J. H. *J. Chem. Phys.* **1988**, *89*, 3789.
(61) Matsumoto, M.; Kataoka, Y. *J. Chem. Phys.* **1988**, *88*, 3233.
(62) Matsumoto, M.; Kataoka, Y. *J. Chem. Phys.* **1989**, *90*, 2398.
(63) Motakabbir, K.; Berkowitz, M. *Chem. Phys. Lett.* **1991**, *176*, 61.
(64) Townsend, R. M.; Rice, S. A. *J. Chem. Phys.* **1991**, *94*, 2207.
(65) Harris, J. G. *J. Phys. Chem.* **1992**, *96*, 5077.
(66) Matsumoto, M.; Takaoka, Y.; Kataoka, Y. *J. Chem. Phys.* **1993**, *98*, 1464.
(67) Benjamin, I. *Phys. Rev. Lett.* **1994**, *73*, 2083.
(68) Linse, P. *J. Chem. Phys.* **1987**, *86*, 4177.
(69) Meyer, M.; Mareschal, M.; Hayoun, M. *J. Chem. Phys.* **1988**, *89*, 1067.
(70) Smit, B. *Phys. Rev. A.* **1988**, *37*, 3431.
(71) Gao, J.; Jorgensen, W. L. *J. Phys. Chem.* **1988**, *92*, 5813.
(72) Carpenter, I. L.; Hehre, W. J. *J. Phys. Chem.* **1990**, *94*, 531.
(73) Smit, B.; Hilbers, P. A. J.; Esselink, K.; Rupert, L. A. M.; van Os, N. M.; Schlijper, A. G. *J. Phys. Chem.* **1991**, *95*, 6361.
(74) Benjamin, I. *J. Chem. Phys.* **1992**, *97*, 1432.
(75) Vanbuuren, A. R.; Marrink, S. J.; Berendsen, H. J. C. *J. Phys. Chem.* **1993**, *97*, 9206.
(76) Michael, D.; Benjamin, I. *J. Phys. Chem.* **1995**, *99*, 1530.
(77) Toxvaerd, S.; Stecki, J. *J. Chem. Phys.* **1995**, *102*, 7163.
(78) Pangali, C.; Rao, M.; Berne, B. J. *J. Chem. Phys.* **1979**, *71*, 2975.
(79) Lee, C. Y.; McCammon, J. A.; Rossky, P. J. *J. Chem. Phys.* **1984**, *80*, 4448.
(80) Spohr, E.; Heinzinger, K. *J. Chem. Phys.* **1986**, *84*, 2304.
(81) Spohr, E.; Heinzinger, K. *Ber. Bunsen-Ges. Phys. Chem.* **1988**, *92*, 1358.
(82) Spohr, E. *J. Phys. Chem.* **1989**, *93*, 6171.
(83) Rossky, P. J.; Lee, S. H. *Chem. Scr.* **1989**, *29A*, 93.
(84) Hautman, J.; Halley, J. W.; Rhee, Y.-J. *J. Chem. Phys.* **1989**, *91*, 467.
(85) Nagy, G.; Heinzinger, K. *J. Electroanal. Chem.* **1990**, *296*, 549.
(86) Heinzinger, K. *Pure Appl. Chem.* **1991**, *63*, 1733.
(87) Watanabe, M.; Brodsky, A. M.; Reinhardt, W. P. *J. Phys. Chem.* **1991**, *95*, 4593.
(88) Raghavan, K.; Foster, K.; Motakabbir, K.; Berkowitz, M. *J. Chem. Phys.* **1991**, *94*, 2110.
(89) Buff, F. P.; Lovett, A. A.; Stillinger, F. H. *Phys. Rev. Lett.* **1965**, *15*, 621.
(90) Sanyal, M. K.; Sinha, S. K.; Huang, K. G.; Ocko, B. M. *Phys. Rev. Lett.* **1991**, *66*, 628.
(91) Weeks, J. D. *J. Chem. Phys.* **1977**, *67*, 3106.
(92) Weeks, J. D. *J. Stat. Phys.* **1991**, *64*, 823.
(93) Requardt, M.; Wagner, H. J. *J. Stat. Phys.* **1991**, *64*, 807.
(94) Romero-Rochin, V.; Varea, C.; Robledo, A. *Physica A* **1992**, *184*, 367.
(95) Iwamatsu, M. *J. Phys. Soc. Jpn.* **1991**, *60*, 1272.
(96) Gomez, M. A.; Chacon, E. *Phys. Rev. B* **1992**, *46*, 723.
(97) Sullivan, D. E.; Levesque, D.; Weis, J. J. *J. Chem. Phys.* **1980**, *72*, 1170.
(98) Lee, L. L. *Molecular Thermodynamics of Nonideal Fluids*; Butterworths: Boston, 1988.
(99) Horn, R. G.; Israelachvili, J. N. *J. Chem. Phys.* **1981**, *75*, 1400.
(100) Israelachvili, J. N. *Adv. Colloid Interface Sci.* **1982**, *16*, 31.
(101) Israelachvili, J. N. *Intermolecular and Surfaces Forces*; Academic Press: London, 1992.
(102) Derjaguin, B. V.; Churaev, N. V. In *Fluid Interfacial Phenomena*; Croxton, C. A., Ed.; Wiley: New York, 1986.
(103) Chandler, D.; Pratt, L. R. *J. Chem. Phys.* **1976**, *65*, 2925.
(104) *Molecular Dynamics in Restricted Geometries*; Klafter, J., Drake, J. K., Eds.; Wiley: New York, 1989.
(105) Granick, S. *Science* **1991**, *253*, 1374.
(106) Berne, B. J.; Borkovec, M.; Straub, J. E. *J. Phys. Chem.* **1988**, *92*, 3711.
(107) Kramers, H. A. *Physica (The Hague)* **1940**, *7*, 284.
(108) Jorgensen, W. L.; Chandresekhar, J.; Madura, J. D.; Impey, R. W.; Klein, M. L. *J. Chem. Phys.* **1983**, *79*, 926.
(109) Stillinger, F. H.; Ben-Naim, A. *J. Chem. Phys.* **1967**, *47*, 4431.
(110) Gubbins, K. E. In *Fluid Interfacial Phenomena*; Croxton, C. A., Ed.; Wiley: New York, 1986.
(111) Croxton, C. A. *Physica A* **1981**, *106*, 239.
(112) Goh, M. C.; Eisenthal, K. B. *Chem. Phys. Lett.* **1989**, *157*, 101.
(113) Wallqvist, A. *Chem. Phys. Lett.* **1990**, *165*, 437.
(114) Thiel, P. A.; Madey, T. E. *Surf. Sci. Rep.* **1987**, *7*, 211.
(115) Spohr, E. *Chem. Phys.* **1990**, *141*, 87.
(116) Schweighofer, K. J.; Benjamin, I. *J. Electroanal. Chem.* **1995**, *391*, 1.
(117) *The Chemical Physics of Solvation;* Dogonadze, R. R., Kalman, E., Kornyshev, A. A., Ulstrup, J., Eds.; Elsevier: Amsterdam, 1988; Part C.
(118) Honig, B. H.; Hubbell, W. L.; Flewelling, R. F. *Annu. Rev. Biophys. Biophys. Chem.* **1986**, *15*, 163.
(119) Saecker, M. E.; Govoni, S. T.; Kowalski, D. V.; King, M. E.; Nathanson, G. M. *Science* **1991**, *252*, 1421.
(120) Saecker, M. E.; Nathanson, G. M. *J. Chem. Phys.* **1993**, *99*, 7056.
(121) King, M. E.; Nathanson, G. M.; Hanning-Lee, M. A.; Minton, T. K. *Phys. Rev. Lett.* **1993**, *70*, 1026.
(122) King, M. E.; Saecker, M. E.; Nathanson, G. M. *J. Chem. Phys.* **1994**, *101*, 2539.
(123) Lipkin, N.; Gerber, R. B.; Moiseyev, N.; Nathanson, G. M. *J. Chem. Phys.* **1994**, *100*, 8408.
(124) Benjamin, I.; Wilson, M. A.; Pohorille, A. *J. Chem. Phys.* **1994**, *100*, 6500.
(125) Benjamin, I.; Wilson, M. A.; Pohorille, A.; Nathanson, G. M. *Chem. Phys. Lett.* **1995**, in press.
(126) Conolly, M. L. *Science* **1983**, *221*, 709.
(127) Chandler, D. *J. Chem. Phys.* **1978**, *68*, 2959.
(128) Rebertus, D. W.; Berne, B. J.; Chandler, D. *J. Chem. Phys.* **1979**, *70*, 3395.
(129) Wilson, M. A.; Chandler, D. *Chem. Phys.* **1990**, *149*, 11.
(130) Scott, T. W.; Liu, J.; Doubleday, C. D., Jr. *Chem Phys.* **1990**, *146*, 327.
(131) Fleming, G. R.; Courtney, S. H.; Balk, M. W. *J. Stat. Phys.* **1986**, *42*, 83.
(132) Straub, J. E.; Borkovec, M.; Berne, B. J. *J. Chem. Phys.* **1988**, *89*, 4833.
(133) Chandler, D.; Pratt, L. R. *J. Chem. Phys* **1976**, *65*, 2925.
(134) Hansen, J.-P.; McDonald, I. R. *Theory of Simple Liquids*, 2nd ed.; Academic Press: London, 1986.
(135) Benjamin, I. *J. Chem. Phys.* **1991**, *94*, 662.
(136) Rose, D. A.; Benjamin, I. *J. Chem. Phys.* **1995**, *102*, 5292.
(137) Berne, B. J.; Tuckerman, M. E.; Straub, J. E.; Bug, A. L. R. *J. Chem. Phys.* **1990**, *93*, 5084.
(138) Grote, R. F.; Zwan, G. v. d.; Hynes, J. T. *J. Phys. Chem.* **1984**, *88*, 4676.
(139) Benjamin, I.; Pohorille, A. *J. Chem. Phys.* **1993**, *98*, 236.
(140) Zichi, D. A.; Rossky, P. J. *J. Chem. Phys.* **1986**, *84*, 1712.
(141) Jorgensen, W. L.; Binning, J. R. C.; Bigot, B. J. *J. Am. Chem. Soc.* **1981**, *103*, 4393.
(142) Jorgensen, W. L. *J. Phys. Chem.* **1983**, *87*, 5304.
(143) Bigot, B.; Costa-Cabral, B. J.; Rivail, J. L. *J. Chem. Phys.* **1985**, *83*, 3083.
(144) Millot, C.; Rivail, J. L. *J. Mol. Liq.* **1989**, *43*, 1.
(145) Torrie, G. M.; Valleau, J. P. *J. Comput. Phys.* **1977**, *23*, 187.
(146) Tanabe, K. *Spectrochim. Acta* **1972**, *28A*, 407.
(147) Pohorille, A.; Wilson, M. A. In *Reaction Dynamics in Clusters and Condensed Phases*; Jortner, J., Levine, R. D., Pullman, B., Eds.; Kluwer: Dordrecht, 1994.
(148) Marcus, Y. *Ion Solvation*; Wiley: New York, 1985.
(149) *The Chemical Physics of Solvation;* Dogonadze, R. R., Kalman, E., Kornyshev, A. A., Ulstrup, J., Eds.; Elsevier: Amsterdam, 1988; Parts A−C.
(150) *Faraday Discuss. Chem. Soc.* **1988**, *85*.
(151) Simon, J. D. *Acc. Chem. Res.* **1988**, *21*, 128.
(152) Bagchi, B. *Annu. Rev. Phys. Chem.* **1989**, *40*, 115.
(153) Maroncelli, M.; MacInnis, J.; Fleming, G. R. *Science* **1989**, *243*, 1674.
(154) Barbara, P. F.; Jarzeba, W. *Adv. Photochem.* **1990**, *15*, 1.
(155) Rossky, P. J.; Simon, J. D. *Nature* **1994**, *370*, 263.
(156) Xiao, X. D.; Vogel, V.; Shen, Y. R.; Marowsky, G. *J. Chem. Phys.* **1991**, *94*, 2315.
(157) Hicks, J. M.; Kemnitz, K.; Eisenthal, K. B.; Heinz, T. F. *J. Phys. Chem.* **1986**, *90*, 560.
(158) Rasing, T.; Berkovic, G.; Shen, Y. R.; Grubb, S. G.; Kim, M. W. *Chem. Phys. Lett.* **1986**, *130*, 1.
(159) Higgins, D. A.; Abrams, M. B.; Byerly, S. B.; Corn, R. M. *Lagmuir* **1992**, *8*, 1994.
(160) Bell, A. J.; Frey, J. G.; Vandernoot, T. J. *J. Chem. Soc., Faraday Trans.* **1992**, *88*, 2027.
(161) Weissbuch, I.; Popovitz-Biro, R.; Wang, J.; Berkovic, G.; Leiserowitz, L.; Lahav, M. *Pure Appl. Chem.* **1992**, *64*, 1263.
(162) Petralli-Mallow, T.; Wong, T. M.; Byers, J. D.; Yee, H. I.; Hicks, J. M. *J. Phys. Chem.* **1993**, *97*, 1383.
(163) Jayne, J. T.; Davidovits, P.; Worsnop, D. R.; Zahniser, M. S.; Kolb, C. E. *J. Phys. Chem.* **1990**, *94*, 6041.
(164) Carnie, S. L.; Torrie, G. M. *Adv. Chem. Phys.* **1984**, *56*, 141.
(165) Blum, L. In *Fluid Interfacial Phenomena*; Croxton, C. A., Ed.; Wiley: New York, 1986.
(166) Blum, L. *Adv. Chem. Phys.* **1990**, *78*, 171.
(167) Bard, A. J. *J. Phys. Chem.* **1993**, *97*, 7147.
(168) Bennett, C. H. In *Algorithms for Chemical Computations*; Christofferson, R. E., Ed.; ACS Symposium Series 46; American Chemical Society: Washington, DC, 1977.
(169) Wilson, M. A.; Pohorille, A.; Pratt, L. R. *Chem. Phys.* **1989**, *129*, 209.
(170) Wilson, M. A.; Pohorille, A. *J. Chem. Phys.* **1991**, *95*, 6005.
(171) Benjamin, I. *J. Chem. Phys.* **1991**, *95*, 3698.
(172) Benjamin, I. *Acc. Chem. Res.* **1995**, *28*, 233.
(173) Randles, J. E. B. *Phys. Chem. Liq.* **1977**, *7*, 107.

(174) Schmickler, W. In *Electrified Interfaces in Physics, Chemistry and Biology*; Guidelli, R., Ed.; Kluwer Academic Publishers: Dordrect, 1992.
(175) Rose, D. A.; Benjamin, I. *J. Chem. Phys.* **1991**, *95*, 6856.
(176) Rose, D. A.; Benjamin, I. *J. Chem. Phys.* **1993**, *98*, 2283.
(177) Seitz-Beywl, J.; Poxleitner, M.; Heinzinger, K. *Z. Naturforsch.* **1991**, *46*, 876.
(178) Glosli, J. N.; Philpott, M. R. *J. Chem. Phys.* **1992**, *96*, 6962.
(179) Matsui, T.; Jorgensen, W. L. *J. Am. Chem. Soc.* **1992**, *114*, 3220.
(180) Perera, L.; Berkowitz, M. L. *J. Phys. Chem.* **1993**, *97*, 13803.
(181) Bockris, J. O'M.; Khan, S. U. M. *Quantum Electrochemistry*; Plenum: New York, 1979.
(182) Tanford, C. *The Hydrophobic Effect*; Wiley: New York, 1981.
(183) Pohorille, A.; Benjamin, I. *J. Chem. Phys.* **1991**, *94*, 5599.
(184) Pohorille, A.; Benjamin, I. *J. Phys. Chem.* **1993**, *97*, 2664.
(185) Zwan, G. v. d.; Hynes, J. T. *J. Chem. Phys.* **1983**, *78*, 4174.
(186) Kosower, E. M.; Huppert, D. *Annu. Rev. Phys. Chem.* **1986**, *37*, 127.
(187) Wolynes, P. G. *J. Chem. Phys.* **1987**, *86*, 5133.
(188) Rips, I.; Klafter, J.; Jortner, J. *J. Chem. Phys.* **1988**, *89*, 4288.
(189) Nichols, A. L.; Calef, D. F. *J. Chem. Phys.* **1988**, *89*, 3783.
(190) Gertner, B. J.; Wilson, K. R.; Zichi, D. A.; Lee, A.; Hynes, J. T. *Faraday Discuss. Chem. Soc.* **1988**, *85*, 297.
(191) Maroncelli, M.; Jr, E. W. C.; Bagchi, B.; Fleming, G. R. *Faraday Discuss. Chem. Soc.* **1988**, *85*, 199.
(192) Carter, E. A.; Hynes, J. T. *J. Chem. Phys.* **1991**, *94*, 5961.
(193) Neria, E.; Nitzan, A. *J. Chem. Phys.* **1992**, *96*, 5433.
(194) Perera, L.; Berkowitz, M. L. *J. Chem. Phys.* **1992**, *96*, 3092.
(195) Frohlich, H. *Theory of dielectrics*; Clarendon: Oxford, 1958.
(196) Maroncelli, M.; Fleming, G. R. *J. Chem. Phys.* **1988**, *89*, 5044.
(197) Maroncelli, M. *J. Chem. Phys.* **1991**, *94*, 2084.
(198) Fonseca, T.; Ladanyi, B. M. *J. Phys. Chem.* **1991**, *95*, 2116.
(199) Chandra, A.; Bagchi, B. *J. Chem. Phys.* **1991**, *94*, 3177.
(200) van der Zwan, G.; Mazo, R. M. *J. Chem. Phys.* **1985**, *82*, 3344.
(201) Girault, H. H. J.; Schiffrin, D. J. In *Electroanalytical Chemistry*; Bard, A. J., Ed.; Dekker: New York, 1989.
(202) Gratzel, M. *Heterogeneous Photochemical Electron Transfer*; CRC Press: Boca Raton, FL, 1989.
(203) Weaver, M. J. *Chem. Rev.* **1992**, *92*, 463.
(204) Gavach, C.; Henry, F. *C. R. Acad. Sci.* **1972**, *C274*, 1545.
(205) Gavach, C. *J. Chim. Phys.* **1973**, *70*, 1478.
(206) Gavach, C.; D'Epenoux, B. *J. Electroanal. Chem.* **1974**, *55*, 59.
(207) Kakiuchi, T.; Senda, M. *Bull. Chem. Soc. Jpn.* **1983**, *56*, 1753.
(208) Hanna, G. J.; Noble, R. D. *Chem. Rev.* **1985**, *85*, 583.
(209) Wandlowski, T.; Marecek, V.; Holub, K.; Samec, Z. *J. Phys. Chem.* **1989**, *93*, 8204.
(210) Sabela, A.; Marecek, V.; Samec, Z.; Fuoco, R. *Electrochim. Acta* **1992**, *37*, 231.
(211) Wandlowski, T.; Marecek, V.; Samec, Z.; Fuoco, R. *J. Electroanal. Chem.* **1992**, *331*, 765.
(212) Samec, Z.; Marecek, V. *J. Electroanal. Chem.* **1992**, *333*, 319.
(213) Kakiuchi, T. *J. Electroanal. Chem.* **1993**, *344*, 1.
(214) Kakiuchi, T.; Takasu, Y. *Anal. Chem.* **1994**, *66*, 1853.
(215) Kakiuchi, T.; Takasu, Y. *J. Electroanal. Chem.* **1995**, *381*, 5.
(216) Kornyshev, A. A.; Volkov, A. G. *J. Electroanal. Chem.* **1984**, *180*, 363.
(217) Gurevich, Y. Y.; Kharkats, Y. I. *J. Electroanal. Chem.* **1986**, *200*, 3.
(218) Samec, Z.; Kharkats, Y. I.; Gurevich, Y. Y. *J. Electroanal. Chem.* **1986**, *204*, 257.
(219) Benjamin, I. *J. Chem. Phys.* **1992**, *96*, 577.
(220) Benjamin, I. *Science* **1993**, *261*, 1558.
(221) Schweighofer, K. J.; Benjamin, I. *J. Phys. Chem.* **1995**, *99*, in press.
(222) Hayoun, M.; Meyer, M.; Turq, P. *J. Phys. Chem.* **1994**, *98*, 6626.
(223) Levy, R. M.; Belhadj, M.; Kitchen, D. B. *J. Chem. Phys.* **1991**, *95*, 3627.
(224) Reiss, H.; Frisch, H. L.; Lebowitz, J. L. *J. Chem. Phys.* **1959**, *31*, 369.
(225) Stillinger, F. H. *J. Solution Chem.* **1973**, *2*, 141.
(226) Pierotti, R. A. *Chem. Rev.* **1976**, *76*, 717.
(227) Benjamin, I. In *Reaction Dynamics in Clusters and Condensed Phases*; Jortner, J., Levine, R. D., Pullman, B., Eds.; Kluwer: Dordrecht, The Netherlands, 1994.
(228) Pohorille, A.; Pratt, L. R. *J. Am. Chem. Soc.* **1990**, *112*, 5066.
(229) Kampen, N. G. V. *Stochastic Processes in Physics and Chemistry;* North-Holland: Amsterdam, 1981.
(230) Marcus, R. A. *J. Chem. Phys.* **1965**, *43*, 679.
(231) Ulstrup, J. *Charge Transfer Processes in Condensed Media*; Springer: Berlin, 1979.
(232) Newton, M. D.; Sutin, N. *Annu. Rev. Phys. Chem.* **1984**, *35*, 437.
(233) Geblewicz, G.; Schiffrin, D. J. *J. Electroanal. Chem.* **1988**, *244*, 27.
(234) Cheng, Y. F.; Schiffrin, D. J. *J. Electroanal. Chem.* **1991**, *314*, 153.
(235) Maeda, K.; Kihara, S.; Suzuki, M.; Matsui, M. *J. Electroanal. Chem.* **1991**, *303*, 171.
(236) Brown, A. R.; Yellowlees, L. J.; Girault, H. H. *J. Chem. Soc. Faraday Trans.* **1993**, *89*, 207.
(237) Kharkats, Y. I.; Volkov, A. G. *J. Electroanal. Chem.* **1985**, *184*, 435.
(238) Kuznetsov, A. M.; Kharkats, Y. I. In *The Interface Structure and Electrochemical Processes at the Boundary Between Two Immiscible Liquids*; Kazarinov, V. E., Ed.; Springer: Berlin, 1987.
(239) Marcus, R. A. *J. Phys. Chem.* **1990**, *94*, 1050, 4152.
(240) Benjamin, I. *J. Phys. Chem.* **1991**, *95*, 6675.
(241) Benjamin, I. In *Structure and Reactivity in Aqueous Solution*; Cramer, C. J., Truhlar, D. G., Eds.; ACS Symposium series 568; American Chemical Society: Washington, DC, 1994.
(242) Benjamin, I. *Chem. Phys.* **1994**, *180*, 287.
(243) Marcus, R. A. *J. Phys. Chem.* **1990**, *94*, 4152.
(244) Marcus, R. A. *J. Phys. Chem.* **1991**, *95*, 2010.
(245) Marcus, R. A. *J. Chem. Phys.* **1963**, *38*, 1858.
(246) Marcus, R. A. *J. Chem. Phys.* **1956**, *24*, 979.
(247) Zener, C. *Proc. R. Soc. London, Ser. A* **1932**, *137*, 696.
(248) Warshel, A. *J. Phys. Chem.* **1982**, *86*, 2218.
(249) Calef, D. F.; Wolynes, P. G. *J. Chem. Phys.* **1983**, *78*, 470.
(250) Hwang, J. K.; Warshel, A. *J. Am. Chem. Soc.* **1987**, *109*, 715.
(251) Kuharski, R. A.; Bader, J. S.; Chandler, D.; Sprik, M.; Klein, M. L.; Impey, R. W. *J. Chem. Phys.* **1988**, *89*, 3248.
(252) Carter, E. A.; Hynes, J. T. *J. Phys. Chem.* **1989**, *93*, 2184.
(253) King, G.; Warshel, A. *J. Chem. Phys.* **1990**, *93*, 8682.
(254) Hynes, J. T.; Carter, E. A.; Ciccotti, G.; Kim, H. J.; Zichi, D. A.; Ferrario, M.; Kapral, R. In *Perspectives in Photosynthesis*; Jortner, J., Pullman, B., Eds.; Reidel: Dordrecht, 1990.
(255) Dogonadze, R. R. In *Reactions of Molecules at Electrodes*; Hush, N. S., Ed.; Wiley: London, 1971.
(256) Schmickler, W. *J. Electroanal. Chem.* **1986**, *204*, 31.
(257) Sebastian, K. L.; Ananthapadmanabhan, P. *J. Electroanal. Chem.* **1987**, *230*, 43.
(258) Kuznetsov, A. M. *J. Electroanal. Chem.* **1988**, *241*, 45.
(259) Sebastian, K. L. *J. Chem. Phys.* **1989**, *90*, 5056.
(260) Gorodyskii, A. V.; Karasevskii, A. I.; Matyushov, D. V. *J. Electroanal. Chem.* **1991**, *315*, 9.
(261) Smith, B. B.; Hynes, J. T. *J. Chem. Phys.* **1993**, *99*, 6517.
(262) Halley, J. W.; Hautman, J. *Phys. Rev. B* **1988**, *38*, 11704.
(263) Curtiss, L. A.; Halley, J. W.; Hautman, J.; Hung, N. C.; Nagy, Z.; Rhee, Y.-J.; Yonco, R. M. *J. Electrochem. Soc.* **1991**, *138*, 2032.
(264) Straus, J. B.; Voth, G. A. *J. Phys. Chem.* **1993**, *97*, 7388.
(265) Rose, D. A.; Benjamin, I. *J. Chem. Phys.* **1994**, *100*, 3545.
(266) Rose, D. A.; Benjamin, I. *Chem. Phys. Lett.* **1995**, *234*, 209.
(267) Xia, X.; Berkowitz, M. L. *Chem. Phys. Lett.* **1994**, *227*, 561.
(268) Hwang, J. K.; Warshel, A. *J. Chem. Phys.* **1986**, *84*, 4938.
(269) Straus, J. B.; Calhoun, A.; Voth, G. A. *J. Chem. Phys* **1995**, *102*, 529.
(270) Price, D. L.; Halley, J. W. *J. Chem. Phys.* **1995**, *102*, 6603.

CR950230+